ISSN: 2164-5388 Volume 10, Number 1, January 2020

Scientific Research Publishing

Open Journal of Biophysics

ISSN: 2164-5388

https://www.scirp.org/journal/ojbiphy

Journal Editorial Board

ISSN Print: 2164-5388 ISSN Online: 2164-5396
https://www.scirp.org/journal/ojbiphy

Associate Editors

Editorial Board

Scientific Research Publishing

Open Journal of Biophysics, 2020, 10, 1-45
https://www.scirp.org/journal/ojbiphy
ISSN Online: 2164-5396
ISSN Print: 2164-5388

Table of Contents

Volume 10 Number 1 January 2020

Open Journal of Biophysics (OJBIPHY)
Journal Information

SUBSCRIPTIONS

The *Open Journal of Biophysics* (Online at Scientific Research Publishing, https://www.scirp.org/) is published quarterly by Scientific Research Publishing, Inc., USA.

Subscription rates:
Print: $79 per issue.
To subscribe, please contact Journals Subscriptions Department, E-mail: sub@scirp.org

SERVICES

Advertisements
Advertisement Sales Department, E-mail: service@scirp.org

Reprints (minimum quantity 100 copies)
Reprints Co-ordinator, Scientific Research Publishing, Inc., USA.
E-mail: sub@scirp.org

COPYRIGHT

PRODUCTION INFORMATION

For manuscripts that have been accepted for publication, please contact:
E-mail: ojbiphy@scirp.org

Scientific Research Publishing

Open Journal of Biophysics, 2020, 10, 1-12
https://www.scirp.org/journal/ojbiphy
ISSN Online: 2164-5396
ISSN Print: 2164-5388

Noises and Signal-to-Noise Ratio of Nanosize EIS and ISFET Biosensors

Lusine Gasparyan[1,2], Ilya Mazo[3], Vahan Simonyan[1], Ferdinand Gasparyan[2*]

[1]DNA-HIVE LLC 15313 Diamond Cove Terrace, Rockville, USA
[2]Yerevan State University, Yerevan, Armenia
[3]Argentis LLC, Gaithersburg, USA
Email: *fgaspar@ysu.am

How to cite this paper: Gasparyan, L., Mazo, I., Simonyan, V. and Gasparyan, F. (2020) Noises and Signal-to-Noise Ratio of Nanosize EIS and ISFET Biosensors. *Open Journal of Biophysics*, **10**, 1-12.
https://doi.org/10.4236/ojbiphy.2020.101001

Received: November 30, 2019
Accepted: December 17, 2019
Published: December 20, 2019

Abstract

The results of comparative theoretical analyzes of the behavior of internal low-frequency noises, signal-to-noise ratio and sensitivity to DNA molecules for EIS and ISFET based nanosize biosensors are presented. It is shown that EIS biosensor is more sensitive to the presence of DNA molecules in aqueous solution than ISFET sensor. Internal electrical noises level decreases with the increase of concentration of DNA molecules in aqueous solution. In the frequency range 10^{-3} - 10^{3} Hz noises level for EIS sensor about in three orders is higher than for ISFET sensor. In the other hand, signal-to-noise ratio for capacitive EIS biosensor is much higher than for ISFET sensor.

Keywords

Biosensor, Noise, Sensitivity, Signal-to-Noise Ratio

1. Introduction

Biosensors based on the field-effect transistors (BioFETs) are potential candidates for future bioassay applications due to its fast response, high sensitivity, high signal-to-noise ratio, small sensing size and low cost. The ion-sensitive field-effect transistors (ISFET) and electrolyte-insulator-semiconductor (EIS) pH-sensitive structures are very important sensors for *in vivo* continuous monitoring application of physiological and environmental mediums and systems. Main types of semiconductor based BioFET sensors operated using peculiarities of field-effect, especially modulation of depletion layer conductance on the semiconductor-other media (metal, dielectric) interface. It is obvious, that sensitivity, selectivity and detectivity of electronic devices, including BioFET sensors, determined in general by the internal electrical noises types, its level and fre-

quency behavior, and consequently by the signal-to-noise ratio (SNR).

Fluctuations in environmental parameters, such as, for example, the concentration and velocity of ions and DNA molecules in an aqueous solution, lead to important random scattering processes that can affect the viability of sequencing. A simple model that captures the role of complex environment in electronic de-phasing and its ability to remove charge carriers from current-carrying states is analyzed in [1]. The environment is composed of ionic, DNA and aqueous solution fluctuations and other random excitations that may drastically affect the electron dynamics, and thus the ionic (or tunnel) current and noise at the DNA detection and sequencing processes [2].

Note that the excess noise level at the DNA sequencing using the solid-state nanopores (which a few tens of pA to 100 pA, 10 times larger than that of protein counterparts [3] [4] [5] [6]) has been one of the key issues responsible for the degraded SNR and temporal and spatial resolution.

Previous theoretical works showed the four DNA nucleotides possess statistically distinguishable electronic signatures in the form of ionic blockade or tunnel current distributions when accounting for structural distortions and partial control of the DNA dynamics [7] [8] [9] [10] [11]. These results indicate DNA sequencing is, in principle, possible via transverse current measurements. However, such studies have neglected scattering processes, such as fluctuations of the environment, which introduce current noise, and may thus affect the ability to distinguish the DNA bases. A solid-state nanopore platform with a low noise level and sufficient sensitivity to discriminate single-strand DNA (ssDNA) homopolymers of poly-A_{40} and poly-T_{40} using ionic current blockade sensing is proposed and demonstrated in [12].

In Ref. [13] the low-frequency pH-dependent electrochemical noise that originates from the ionic conductance of the electrode-electrolyte-FET structure of the device and that the noise depends on the concentration of the electrolyte and $1/f$ in nature are investigated. The statistical and frequency analysis of this electrochemical noise of a commercial ISFET sensor, under room temperature has been performed for different pH values. It is also proposed a concentration dependent a/f and b/f^2 model of the noise with different values of the coefficients a and b (here f is the frequency).

The numerical and analytical theory of signal and noise of double-gated pH-sensors was provided in [14]. The transport and noise properties of an array of silicon nanowire FET sensors are investigated in [15]. It is shown that drain current substantially depends on pH value and SNR reaches the high value of 10^5. The noise characteristic index decreases from 1.1 to 0.7 with the growth of the liquid gate voltage. Noise behavior is successfully explained in the framework of the correlated number-mobility unified fluctuation model.

To explain the nature and behavior of $1/f$ -noise in devices based on FET, the following basic theories and models are proposed: the carrier density or number fluctuation model introduced by McWhorter [16], the carriers mobil-

ity fluctuation model proposed by Hooge empirical relation [17], the electron-phonon interaction model [18] [19] [20] [21] and the charge fluctuation model [22] [23] proposed by us.

The accuracy of ISFET output measurement is greatly affected by the presences of internal noises, drift, diffusion and slow response of the device. Although the noise analysis of ISFETs so far performed in different literature relates only to sources originated from FET structure which is almost constant for a particular device, the pH, or charged DNA molecules concentration dependent electrochemical noise has not been substantially explored and analyzed in detail.

As usually the time constants involved in the detection of biological and chemical species in electrolyte medium via field effect are relatively large, it would be expected that low-frequency noise is more critical than other types of noises in BioFET sensors. Therefore, further we will analyze just low-frequency $1/f$ -noise behavior.

In this paper the results of theoretical simulation of the behavior and peculiarities of low-frequency $1/f$ -noise and signal-to-noise ratio for nanosize BioFET sensors are presented. Numerical simulation of the noise spectral density and signal-to-noise ratio we do for EIS and ISFET sensors based on the silicon (as semiconductor) and silicon dioxide (as insulator).

2. Low-Frequency Noises in BioFET Sensors

The detailed analysis shows that main types of electrical noises in BioFET sensors can be classified as follows [24]-[29]:

1) Noise generated in solid state part of the sensor

- Thermal noise;
- Generation-recombination (g-r) noise in the space charge region at the substrate-channel interface;
- $1/f$ -and g-r noises generated due to trapping and detrapping on the semiconductor-insulator interface;
- Hooge's bulk $1/f$ -noise in semiconductor;
- Current channel $1/f$ -noise.

2) Electrochemical noise associated with the ion/charged molecules-insulator interactions

- Thermal noise;
- $1/f$ -noise in corrosive interfaces;
- Shot or Schottky noise;
- Spurious noise.

3) Noise generated in the aqueous solution and at the reference electrode as well as noise resulting from the fluctuations of the biasing elements

- Bulk thermal noise;
- Diffusion layer thermal noise;
- $1/f$ -noise in corrosive interfaces;
- Biological noise.

Low-frequency noise conditioned by the random fluctuations of concentration or mobility of current carriers, ions and charged DNA molecules in aqueous solution, by the trapping-detrapping processes on the surface and interface states, by the electron-phonon interactions, as well as by the fluctuation of electron's and phonon's distribution functions in the bulk of semiconductor. As already noted, for BioFET sensors low-frequency noise is of greater interest, which, as a rule, can be determined and explained using the Hooge's model [21] [30] [31] [32], McWhorter or correlated number-mobility fluctuation model [16] [33] [34] and charge fluctuation model [22].

For the linear regime of operation of BioFETs signal-to-noise ratio can be calculated using expressions:

$$SNR = \frac{I_S}{I_N} = \frac{I_S}{\sqrt{S_I \Delta f}}, \tag{1a}$$

or

$$= \frac{V_S}{V_N} = \frac{V_S}{\sqrt{S_V \Delta f}}. \tag{1b}$$

Here I_S (V_S) and I_N (V_N) are useful signal current (voltage) and noise equivalent current (voltage), correspondingly, S_I (S_V) are current (voltage) noise spectral densities, Δf is the frequency bandwidth. In numerical calculations we take $\Delta f = 1\,\text{Hz}$.

2.1. EIS Biosensor

It is clear that for EIS biosensors main physical effects that influence on the low-frequency noise behavior is carried out in the interface electrolyte-insulator (see Figure 8b in [35]). As EIS is the capacitive device the main type of electrical noise must be connected with capacitance (or charge) random fluctuation. At such situation dominant noise type will be noise conditioned by the oxide (insulator) surface charge fluctuation. We will take accounts that the oxide surface charge is changed during the DNA sensing processes. This is occurring by the capture of negatively charged DNA molecules on the proton acceptor OH_2^+ bonds and the capture of H^+ ions (protons) of the solution on the proton donor free OH^- bonds on the interface solution-insulator (see Figure 2 in [7], and [36]). These are molecules and ions located at a distance of Debye length from the oxide surface. Thus, to calculate noise spectral density, we can use an expression that takes into account charge fluctuations [37]:

$$S_V(f) = \frac{S_Q(f)}{C_{ef}^2} = \frac{e^2 N_t}{wlC_{ef}^2}\frac{1}{f}. \tag{2}$$

Here $S_Q(f)$ is the noise spectral density conditioned by charge fluctuation, N_t is the equivalent total density of traps per unit area at the SiO_2/electrolyte interface, w and l are width and length of the sensitive oxide layer, correspondingly, f is the frequency, $C_{ef} = \frac{C_{ox}C_d}{C_{ox}+C_d}$, C_{ox} and C_d are the capaci-

tances per unit area of the insulator layer and the semiconductor depletion layer, correspondingly:

$$C_{ox} = \frac{\varepsilon_0 \varepsilon_{ox}}{t_{ox}}, \quad C_d = \frac{\varepsilon_0 \varepsilon_{Si}}{t_d}.$$

Here ε_0, ε_{ox} and ε_{Si} are dielectric permittivity of free space, insulator and semiconductor, t_{ox} and t_d are thicknesses of insulator and semiconductor depletion layers, correspondingly. For simplicity assume that before fill the aqueous solution by the DNA molecules, the proton donor OH^- bonds in SiO_2/electrolyte interface was fully compensated (passivized) by the protons of the solution and in further do not participate on the surface charge changing process. Therefore the oxide surface charge per unit area conditioned only by proton acceptor OH_2^+ bonds ($Q_{ox} = qN_t^+$) will be changed only at the capture of negatively charged DNA molecules. So it becomes (see [7] [36]):

$$Q'_{ox} = qN_t^+ (1-\delta), \quad \delta \equiv \frac{N_{DNA}}{N_t^+}. \tag{3}$$

Here N_t^+ is the concentration of the proton acceptor traps on the unit area of oxide surface, N_{DNA} is the DNA surface concentration in solution near the oxide at a distance of the Debye length (see also [7]). Thus Equation (2) will be changed as follows:

$$S_V(f) = \frac{e^2 N_t^+ (1-\delta)}{wlC_{ef}^2} \frac{1}{f}. \tag{4}$$

For numerical simulation we used following parameters: $t_d = 2\times10^{-6}$ cm, $t_{ox} = 10^{-6}$ cm, $\varepsilon_{Si} = 11.7$, $\varepsilon_{ox} = 3.9$, $\varepsilon_0 = 8.85\times10^{-14}$ F/cm, $w = 1.5\times10^{-6}$ cm; $l = 2\times10^{-6}$ cm. For the value of N_t^+ we can do following estimation. Assume that traps concentration on the interface SiO_2-electrolyte same than SiO_2-Si interface. According data [7] [37] traps concentration in Si-SiO_2 interface is about (10^{10} - 10^{11}) cm^{-2}. In the numerical calculations we will use $N_t^+ \approx 10^{11}\,cm^{-2}$. For C_{ef} we have $C_{ef} \approx 2.1\times10^{-5}\,F/cm^2$.

As we can see from expression (4) increase of the sensitive surface area (wl) brings to decrease of the noise level. On the other hand it is well known that increase of sensitive surface brings to increase of sensitivity of the BioFET to DNA molecules (see also [7]). At the same time, for low noise and high sensitivity, sensors with a relatively large surface area should be used.

In **Figure 1** spectral dependency of low-frequency noise for EIS biosensor is presented for different values of DNA concentration (or δ) in logarithmic scale. Noises level decrease with increasing of the DNA concentration. Such behavior can be explained as follows. Increasing of the DNA molecules number near oxide surface brings to partially compensation of surface positive charge. As a result charge fluctuation level and consequently noise spectral density of this charge is decrease.

As it is follow from Equation (4) at the completely compensation (passivation) of oxide surface charge ($\delta = 1$) noise density of charge fluctuation becomes to

zero. Now total noise will be determined by the other types of noises (thermal, $1/f$ -noise in corrosive interfaces, spurious noise). Dependencies of noise level from DNA molecules concentration (or δ) presented in Figure 2. Noise spectral density decreases when DNA concentration is increase. As it is shown in

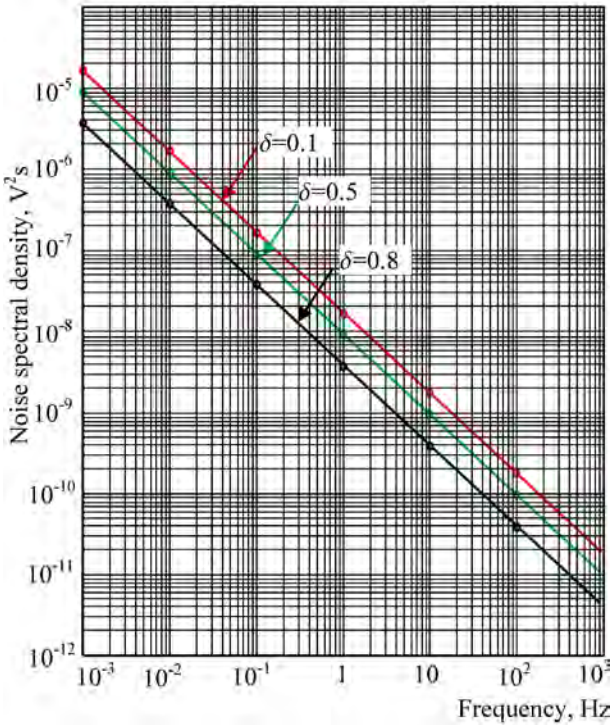

Figure 1. Low-frequency noise spectral dependency for EIS biosensor. The graphs are built according Equation (4).

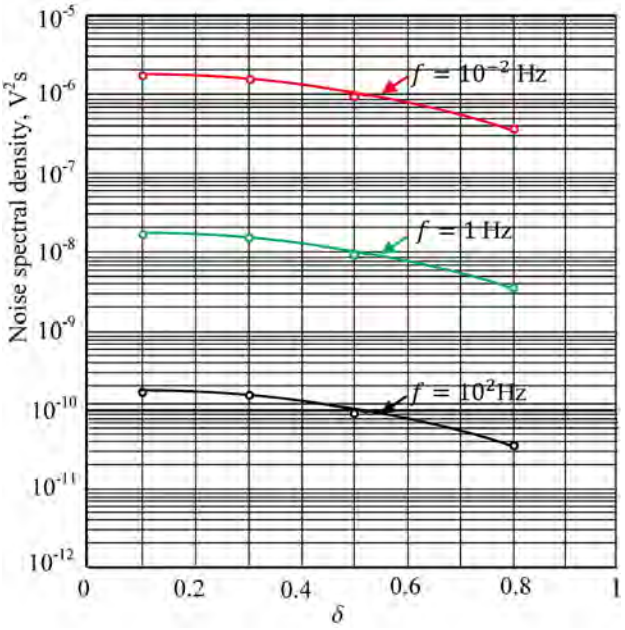

Figure 2. Dependency of noise spectral density for EIS biosensor vs. concentration of DNA molecules.

Figure 3 for the parameters (sizes) of the EIS biosensor selected above SNR can reach high values up to 10^5 - 10^6. Note that SNR is calculated according to formula (1b).

2.2. ISFET Biosensor

The main physical processes that occur in ISFET sensors and affect the response of the device to the presence of DNA molecules in an aqueous solution and to the source of generated noise in the channel occur mainly in the current channel between sources and drain electrodes (see Figure 1a in [7]). Fluctuation of the source-drain current besides carrier's concentration and mobility fluctuation is conditioned also by the fluctuation (change) of the semiconductor surface potential that depends on concentration of DNA molecules in aqueous solution via charge fluctuation in SiO_2/electrolyte interface [7] [36]. According to Hooge's empirical mobility fluctuation model low-frequency noise for ISFET sensor can be presented by the following expression:

$$S_i(f) = \frac{e\alpha_H I_{sd}}{wlC_{ox}\left(V_g - V_{th}\right)}\frac{1}{f}. \tag{7}$$

Here V_g and V_{th} are gate[1] and threshold voltages, I_{sd} is the source-drain current of field-effect transistor, α_H is the Hooge's parameter. For ISFET biosensor in [7] we obtain an expression for the source-drain current, which, in addition to the electrical and structural parameters of the semiconductor, also depends on the surface potential of current channel (semiconductor depletion layer) (see Equation (3) in [7]). After some modifications, source-drain current can be represented by the following form:

$$I_{sd} \approx \frac{et_d wn_0 V_{ds}}{l\varphi_T}\left[\mu_0 - \theta\left(V_g + 2\varphi_F + \phi_{dl} - \frac{\Phi_{Si} - \Phi_{ox}}{q} + \frac{Q_{ox}}{C_{ox}}\right)\right] \times\left[\varphi_T\left(1 + \ln\frac{B}{2}\right) + V_g + 2\varphi_F + \phi_{dl} - \frac{\Phi_{Si} - \Phi_{ox}}{q} + \frac{Q_{ox}}{C_{ox}}\right]. \tag{8}$$

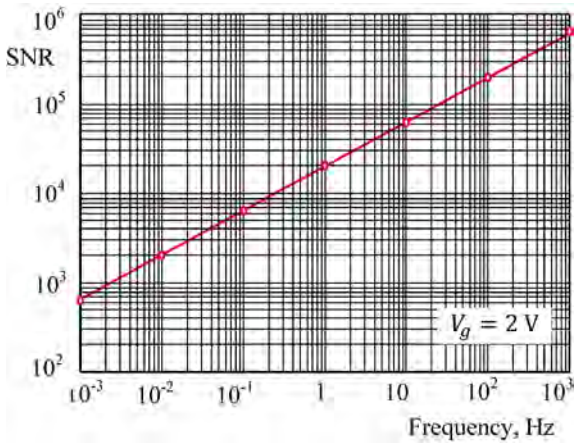

Figure 3. Frequency dependency of SNR for EIS biosensor at the gate voltage 2 V.

[1]Under gate voltage we mean voltage applied between reference electrode and source electrode.

Here

$$\varphi_F = 2\varphi_T \ln\frac{N_A}{n_i},\quad \varphi_T = \frac{k_B T}{q},\quad \phi_{dl} = 2\varphi_T\left(\frac{\varepsilon_w}{\varepsilon_r}\frac{N_{sol}}{K_{AK}^{+}+H_s^{+}}\right);\quad \phi_{ox} = \frac{qN_t}{C_{ox}},$$

$$C_{ox} = \frac{\varepsilon_0\varepsilon_{ox}}{t_{ox}};\quad B \equiv \frac{\varphi_T\varepsilon_0\varepsilon_{ox}N_A}{qt_{ox}^2 n_i^2}.$$

Here ϕ_{ox} and ϕ_{dl} are potentials of the oxide layer and double layer, correspondingly, Φ_{Si} and Φ_{ox} are the work functions of silicon and silicon dioxide (SiO_2), correspondingly; V_{ds} is the source-drain voltage, Q_{ox} is the oxide layer charge per unit area, C_{ox} is the capacitance of the oxide layer per unit area; ε_w and ε_r are the dielectric permittivity of water and electrolyte, respectively; N_A is the doping acceptor concentration in p-Si substrate; n_i is the intrinsic carrier concentration in bulk silicon, n_0 and p_0 ($p_0 \approx N_A$) are the equilibrium electron and hole concentrations in semiconductor, K_{AK}^{+} is the molar concentration of the cations in the solution, H_s^{+} is the molar concentration of the hydrogen ions (protons) at the oxide surface, k_B is the Boltzmann constant, T is the absolute temperature, μ_0 is the low-field magnitude of the mobility of carriers, θ is the some constant.

For numerical simulation besides of parameters presented above for EIS sensor we use also following additional parameters: $\mu_0 = 260\ \mathrm{cm^2/(V\cdot s)}$ [38], $\theta = 28\ \mathrm{cm^2/(V^2\cdot s)}$ [39] [40] [41], $\varphi_T = 0.026$ V, $N_{sol} = 0.015$ mol/l [41], $K_{AK}^{+} = 0.001$ mol/l [41], $\varepsilon_w \approx 80$, $\varepsilon_r \approx 78$, $\Phi_{Si} = 4.85$ eV [37], $\Phi_{ox} = 5$ eV [37], $N_A = 10^{15}\ \mathrm{cm^{-3}}$, $N_V = 2.5\times10^{19}\ \mathrm{cm^{-3}}$ ($m_n^* = m_p^* \equiv m_0 = 9.1\times10^{-31}$ kg, m_n^* and m_p^* are effective mass of electrons and holes, m_0 is the free electron mass).

In Figure 4 spectral dependency of low-frequency noise for ISFET biosensor

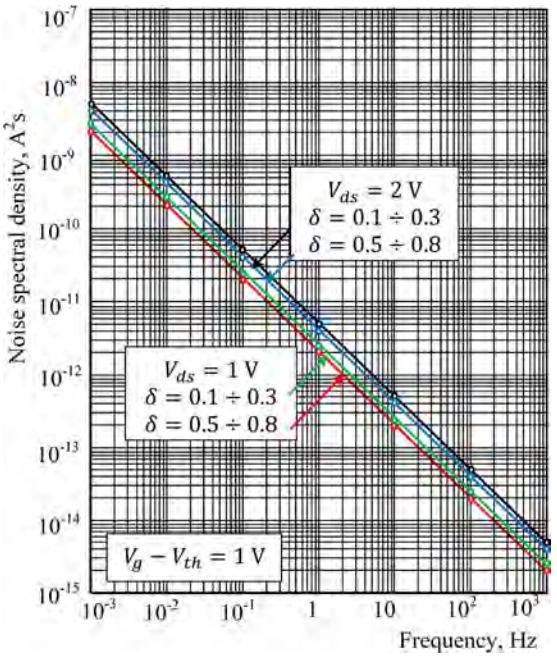

Figure 4. Spectral dependency of noise spectral density for ISFET biosensor according Equation (7).

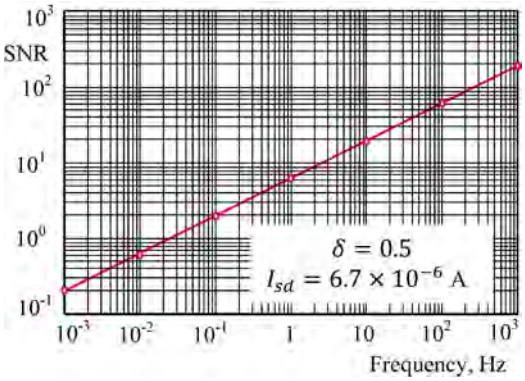

Figure 5. Frequency dependency of signal-to-noise ratio for ISFET biosensor.

are presented in logarithmic scale. Increasing both source-drain voltage and concentration of DNA molecules brings to weak grow of the noise level. Magnitude of the signal-to-noise ratio for ISFET sensor in several orders is smaller than for EIS sensor (see **Figure 3** and **Figure 5**).

3. Conclusion

EIS biosensor is more sensitive to DNA molecules than ISFET sensor. It is conditioned by the more strong modulation of the oxide charge (EIS capacitance) in comparison with weak modulation of the source-drain current of ISFET under influence of DNA molecules. Low-frequency noises level decreases with increasing of concentration of DNA molecules in solution. Such behavior conditioned by the growing dependency of source-drain current with increase of concentration of DNA molecules[2]. High sensitivity of the EIS biosensor conditioned by the "deep modulation" of the charge of oxide layer and consequently by the deep modulation of the EIS totals capacitance under influence of charged DNA molecules in aqueous solution.

Author Contribution Information

All authors participated in the statement of the problem and discussion of the results. L. Gasparyan, and F. Gasparyan conducted a literature review. F. Gasparyan and V. Simonyan made calculations and participated in the writing of the text of the article.

Conflicts of Interest

The authors declare no conflicts of interest regarding the publication of this paper.

References

[1] Krems, M., Zwolak, M., Pershin, Y.V. and Di Ventra, M. (2009) Effect of Noise on DNA Sequencing via Transverse Electronic Transport. *Biophysical Journal*, **97**, 1990-1996. https://doi.org/10.1016/j.bpj.2009.06.055

[2]Explanation of such behavior gives in Ref. [2].

[2] Di Ventra, M. (2008) Electrical Transport in Nanoscale Systems. Cambridge University Press, Cambridge. https://doi.org/10.1017/CBO9780511755606

[3] Wanunu, M., Dadosh, T., Ray, V., Jin, J., McReynolds, L. and Dmdich, M. (2010) Rapid Electronic Detection of Probe-Specific microRNAs Using Thin Nanopore Sensors. *Nature Nanotechnology*, **5**, 807-814. https://doi.org/10.1038/nnano.2010.202

[4] Garaj, S., Hubbard, W., Reina, A., Kong, J., Branton, D. and Golovchenko, J.A. (2010) Graphene as a Subnanometre Trans-Electrode Membrane. *Nature*, **467**, 190-193. https://doi.org/10.1038/nature09379

[5] Merchant, C.A., Healy, K., Wanunu, M., *et al.* (2010) DNA Translocation through Graphene Nanopores. *Nano Letters*, **10**, 2915-2921. https://doi.org/10.1021/nl101046t

[6] Schneider, G.F., Kowalczyk, S.W., Calado, V.E., Pandraut, G., *et al.* (2010) DNA Translocation through Graphene Nanopores. *Nano Letters*, **10**, 3163-3167. https://doi.org/10.1021/nl102069z

[7] Gasparyan, L., Mazo, I., Simonyan, V. and Gasparyan, F. (2019) ISFET Based DNA Sensor: Current-Voltage Characteristic and Sensitivity. *Open Journal of Biophysics*, **9**, 239-253. https://doi.org/10.4236/ojbiphy.2019.94017

[8] Zwolak, M. and Di Ventra, M. (2005) Electronic Signature of DNA Nucleotides via Transverse Transport. *Nano Letters*, **5**, 421-424. https://doi.org/10.1021/nl048289w

[9] Lagerqvist, J., Zwolak, M. and Di Ventra, M. (2006) Fast DNA Sequencing via Transverse Electronic Transport. *Nano Letters*, **6**, 779-782. https://doi.org/10.1021/nl0601076

[10] Lagerqvist, J., Zwolak, M. and Di Ventra, M. (2007) Influence of the Environment and Probes on Rapid DNA Sequencing via Transverse Electronic Transport. *Biophysical Journal*, **93**, 2384-2390. https://doi.org/10.1529/biophysj.106.102269

[11] Lagerqvist, J., Zwolak, M. and Di Ventra, M. (2007) Comment on Characterization of the Tunneling Conductance across DNA Bases. *Physical Review E*: *Statistical*, *Nonlinear*, *and Soft Matter Physics*, **76**, Article ID: 013901. https://doi.org/10.1103/PhysRevE.76.013901

[12] Lee, M.-H., Kumar, A., Park, K.-B., Cho, S.-Y., Kim, H.-M., Lim, M.-C., Kim, Y.-R. and Kim, K.-B. (2014) A Low-Noise Solid-State Nanopore Platform Based on a Highly Insulating Substrate. *Scientific Reports*, **4**, Article No. 7448. https://doi.org/10.1038/srep07448

[13] Das, M.P. and Bhuyan, M. (2013) Modeling of pH Dependent Electrochemical Noise in Ion Sensitive Field Effect Transistors ISFET. *Sensors and Transducers*, **149**, 102-108. https://doi.org/10.4236/mnsms.2014.43013

[14] Tsividis, Y. (1999) Operation and Modeling of the MOS Transistor. 2nd Edition, McGraw-Hill, New York.

[15] Gasparyan, F., Khondkaryan, H., Arakelyan, A., Zadorozhnyi, I., Pud, S. and Vitusevich, S. (2016) Double-Gated Si NW Sensors: Low-Frequency Noise and Photoelectric Properties. *Journal of Applied Physics*, **120**, Article ID: 064902(1-8). https://doi.org/10.1063/1.4960704

[16] McWhorter, A.L. (1957) 1/f Noise and Germanium Surface Properties. In: Kingston, R.H., Ed., *Semiconductor Surface Physics*, University of Pennsylvania Press, Philadelphia, 207-228.

[17] Hooge, F.N. (1993) 1/f Noise Sources. *IEEE Transactions on Electron Devices*, **41**, 1926-1935. https://doi.org/10.1109/16.333808

[18] Gasparyan, F.V., Melkonyan, S.V. and Asriyan, H.V. (2005) Space Confined and Bulk Temporal Fluctuations of Phonons and Linkage between Two Models of 1/f Noise in Semiconductors. *Semiconductor Micro- and Nano-Electronics*, Aghveran, 16-18 September 2005, 24-27.

[19] Melkonyan, S.V., Gasparyan, F.V., Aroutiounian, V.M. and Asriyan, H.V. (2005) 1/f Type Noise in View of Phonons Interface Percolation Dynamics. *Noise and Fluctuations*, Salamanca, 19-23 September 2005, Vol. 780, 87-91. https://doi.org/10.1063/1.2036705

[20] Melkonyan, S.V., Aroutiounian, V.M., Gasparyan, F.V. and Asriyan, H.V. (2006) Phonon Mechanism of Mobility Equilibrium Fluctuation and Properties of 1/f-Noise. *Physica*, *B*: *Physics of Condensed Matter*, **382**, 65-70. https://doi.org/10.1016/j.physb.2006.01.521

[21] Melkonyan, S.V., Gasparyan, F.V. and Asriyan, H.V. (2007) Main Sources of Electron Mobility Fluctuations in Semiconductors. *SPIE* 4*th International Symposium Fluctuation and Noise*, Florence, 20-24 May 2007, Vol. 6600, 66001K-(1-8).

[22] Gasparyan, F.V., Vitusevich, S.A., Offenhäusser, A. and Schöning, M.J. (2011) Modified Charge Fluctuation Noise Model for Electrolyte-Insulator-Semiconductor Devices. *Modern Physics Letters B*, **25**, 831-840. https://doi.org/10.1142/S0217984911026103

[23] Gasparyan, F.V. and Aroutiounian, V.M. (2015) Quantum Modulation of the Channel Charge and Distributed Capacitance of Double Gated Nanosize FETs. *Advances in Nano Research*, **3**, 49-54. https://doi.org/10.12989/anr.2015.3.1.049

[24] Hassibi, A., Navid, R., Dutton, R.W. and Lee, T.H. (2004) Comprehensive Study of Noise Processes in Electrode Electrolyte Interfaces. *Journal of Applied Physics*, **96**, 1074-1082. https://doi.org/10.1063/1.1755429

[25] Tyagai, V.A. (1971) Faradaic Noise of Complex Electrochemical Reactions. *Electrochimica Acta*, **16**, 1647-1654. https://doi.org/10.1016/0013-4686(71)85075-2

[26] Deen, M.J., Shinwari, M.W. and Ranuarez, J.C. (2006) Noise Considerations in Field-Effect Biosensors. *Journal of Applied Physics*, **100**, Article ID: 074703(1-8). https://doi.org/10.1063/1.2355542

[27] Massobrio, G., Martinoa, S. and Grattarola, M. (1992) Light-Addressable Chemical Sensors: Modeling and Computer Simulations. *Sensors and Actuators B*, **7**, 484-487. https://doi.org/10.1038/nchembio.611

[28] Gasparyan, F.V. (2010) Excess Noises in (Bio-)chemical Nanoscale Sensors. *Sensors & Transducers Journal*, **122**, 72-84.

[29] Hassibi, A., Zahedi, S., Navid, R., Dutton, R.W. and Lee, T.H. (2005) Biological Shot-Noise and Quantum-Limited Signal-to-Noise Ratio in Affinity-Based Biosensors. *Journal of Applied Physics*, **97**, Article ID: 084701(1-9). https://doi.org/10.1063/1.1861970

[30] Hooge, F.N. (1969) 1/f Noise Is No Surface Effect. *Physics Letters A*, **29**, 139-140. https://doi.org/10.1016/0375-9601(69)90076-0

[31] Hooge, F.N., Kleinpenning, T.G.M. and Vandamme, L.K.J. (1981) Experimental Studies on 1/f Noise. *Reports on Progress in Physics*, **44**, 479-532. https://iopscience.iop.org/article/10.1088/0034-4885/44/5/001/pdf https://doi.org/10.1088/0034-4885/44/5/001

[32] Hung, K.K., Ko, P.K., Hu, C. and Cheng, Y.C. (1990) A Unified Model for the Flicker Noise in Metal-Oxide-Semiconductor Field-Effect Transistors. *IEEE Transactions on Electron Devices*, **37**, 654-665. https://doi.org/10.1109/16.47770

[33] Christensson, S., Lundström, I. and Svensson, C. (1968) Low Frequency Noise in

MOS Transistors I. Theory. *Solid-State Electronics*, **11**, 797-812. https://doi.org/10.1016/0038-1101(68)90100-7

[34] Christensson, S. and Lundström, I. (1968) Low Frequency Noise in MOS Transistors II. Experiments. *Solid-State Electronics*, **11**, 813-820. https://doi.org/10.1016/0038-1101(68)90101-9

[35] Gasparyan, L., Mazo, I., Simonyan, V. and Gasparyan, F. (2019) DNA Sequencing: Current State and Prospects of Development. *Open Journal of Biophysics*, **9**, 169-197. https://doi.org/10.4236/ojbiphy.2019.93013

[36] Gasparyan, L., Mazo, I., Simonyan, V. and Gasparyan, F. (2020) EIS Biosensor for Detection of DNA Low Concentration. *Journal of Contemporary Physics* (*Armenian Academy of Sciences*). (In Press)

[37] Pantelides, S.T., Wang, S., Franceschetti, A., *et al.* (2006) Si/SiO_2 and SiC/SiO_2 Interfaces for MOSFETs—Challenges and Advances. *Materials Science Forum*, **527-529**, 935-948.

[38] Jeong, C., Antoniadis, D. and Lundstrom, M.S. (2009) On Backscattering and Mobility in Nanoscale Silicon MOSFETs. *IEEE Transactions on Electron Devices*, **56**, 2762-2769. https://doi.org/10.1109/TED.2009.2030844

[39] Park, C., Lee, C., Lee, K., Moon, B.-J., Byun, Y.H. and Shur, M. (1991) A Unified Current-Voltage Model for Long-Channel nMOSFETs. *IEEE Transactions on Electron Devices*, **38**, 399-406. https://doi.org/10.1109/16.69923

[40] Gildenblat, G.S. and Huang, C.-L. (1989) Engineering Model of Inversion Channel Mobility for 60-300k Temperature Range. *Electronics Letters*, **25**, 634-636. https://doi.org/10.1049/el:19890430

[41] Pud, S., Gasparyan, F., Petrychuk, M., Li, J., Offenhausser, A. and Vitusevich, S.A. (2014) Single Trap Dynamics in Electrolyte-Gated Si-Nanowire Field Effect Transistors. *Journal of Applied Physics*, **115**, Article ID: 233705(1-11). https://doi.org/10.1063/1.4960704

Scientific Research Publishing

Open Journal of Biophysics, 2020, 10, 13-26
https://www.scirp.org/journal/ojbiphy
ISSN Online: 2164-5396
ISSN Print: 2164-5388

The Radioactive ^{45}Ca Cannot Be Used for Adequate Estimation of the Functional Activity of ^{40}Ca Ions in Cells and Organisms

Anna Nikoghosyan, Lilia Narinyan, Armenuhi Heqimyan, Sinerik Ayrapetyan*

Life Sciences International Postgraduate Educational Center, UNESCO Chair in Life Sciences, Yerevan, Armenia
Email: *info@biophys.am

How to cite this paper: Nikoghosyan, A., Narinyan, L., Heqimyan, A. and Ayrapetyan, S. (2020) The Radioactive ^{45}Ca Cannot be Used for Adequate Estimation of the Functional Activity of ^{40}Ca Ions in Cells and Organisms. *Open Journal of Biophysics*, **10**, 13-26.
https://doi.org/10.4236/ojbiphy.2020.101002

Received: December 12, 2019
Accepted: January 13, 2020
Published: January 16, 2020

Abstract

Previously we have shown that nM ouabain-induced activation of cAMP-dependent Na/Ca exchange in reverse (R) mode in cell membrane has age-dependent weakening hydration effect on heart muscle and brain tissues and such Na/Ca exchange is characterized by quantum mechanical sensitivity. As in biological experiments radioactive ^{45}Ca is used for the study of cold ^{40}Ca exchange in cells and organisms, in the present work, the age-dependent effect of physiological solution (PS) containing either ^{40}Ca or ^{45}Ca on tissue hydration in different experimental conditions was studied in order to evaluate the bioequivalence of these two forms of Ca. The obtained data indicate that the intraperitoneal injections of ^{40}Ca PS and ^{45}Ca PS leading to activation of RNa/^{40}Ca and RNa/^{45}Ca exchanges, respectively, have different age-dependent effects on heart muscle and brain tissue hydration. As in myocyte membrane, the Na/Ca exchange is more expressed than in neuronal membrane, the age-dependent heart muscle hydration is more sensitive to quantum properties of Ca than brain tissue hydration. The $[^{45}Ca]_i$, in contrary to $[^{40}Ca]_i$, has age-dependent weakening and stabilizing effect on tissue hydration and makes the latter insensitive to ouabain. The obtained data bring us to a strong conclusion that RNa/Ca exchange has quantum mechanical properties and in biological experiments radioactive ^{45}Ca cannot be used for adequate estimation of the functional activity of ^{40}Ca ions in cells and organisms.

Keywords

Rat, Brain, Heart Muscle, ^{45}Ca, Na/Ca Exchange, Ouabain

1. Introduction

Metabolic control of cell hydration is a fundamental parameter determining its

functional activity. Our previous study has shown that the metabolically driven water efflux from the cell is a key mechanism controlling low membrane permeability for Na ions and membrane excitability [1]. Traditionally, the age-dependent increase of intracellular Ca ($[Ca]_i$) contents is considered as a result of activation of Na/Ca exchange in reverse (R) mode in response to Na/K pump dysfunction-induced increase of intracellular Na ($[Na]_i$) [2] [3]. However, we have shown that the activation of RNa/Ca exchange, occurring also upon the impact of extremely weak chemical and physical factors, is unable to change the Na/K pump and ionic channel activities in membrane, which are due to the increase of intracellular cAMP contents [4] [5] [6] [7] [8]. It is notable that, in spite of the fact that RNa/Ca exchange functions in stoichiometry of 3Na:1Ca, its activation, as a result of Na gradient decrease, only leads to cell dehydration, while in case of activation of cAMP-dependent decrease of intracellular Ca ($[Ca]_i$) contents, it has age-dependent weakening hydration effect on heart and brain tissues [9] [10].

Thus, on the basis of the above presented and literature data on the key role of intracellular messengers in regulation of $[Ca]_i$, the cGMP/cAMP-dependent Na/Ca exchange has been suggested as a universal membrane sensor through which the biological effects of weak signals on excitable cells are realized [8] [11] [12].

Our recent studies show that cAMP-dependent RNa/Ca exchange-induced cell hydration has quantum mechanical sensitivity: pM and nM radioactive [^{3}H]-ouabain modulate brain tissue hydration more effectively than the same doses of non-labeled (cold) ouabain [13]. Considering the fact that radioactive ^{45}Ca is widely used for the study of cold ^{40}Ca exchange in cells and organisms, it seems extremely important to evaluate the diversity of their functional activities. It is suggested that the comparative study of age-dependent effects of RNa/Ca exchange on heart muscle hydration (contraction) and brain tissue hydration after intraperitoneal (i/p) injections of physiological solution (PS) containing cold ^{40}Ca and radioactive ^{45}Ca could help to reveal the mechanism(s) through which the ^{45}Ca modulates heart muscle and brain tissue hydration. For this purpose, in the present work, the comparative study of age-dependent effects of RNa/^{40}Ca and RNa/^{45}Ca exchange on heart muscle and brain tissue hydration and ^{45}Ca uptake in different experimental conditions were performed.

2. Materials and Methods

2.1. Animals

All procedures performed on animals were carried out following the protocols approved by Animal Care and Use Committee of Life Sciences International Postgraduate Educational Centre (LSIPEC, Yerevan, Armenia).

The experiments were performed on young (6 weeks old) and old (18 months old) mail albino rats. They were regularly examined, kept under control of the veterinarians in LSIPEC and reserved in a specific pathogen-free animal room

under optimum conditions of 12 h light/dark cycles, at temperature of 22˚C ± 2˚C, with a relative humidity of 50% and were fed *ad libitum* on a standard lab chow and water.

2.2. Chemicals

Tyrode's PS containing (in mM) 137 NaCl, 5.4 KCl, 1.8 $CaCl_2$, 1.05 $MgCl_2$, 5 $C_6H_{12}O_6$, 11.9 $NaHCO_3$, and 0.42 NaH_2PO_4 and adjusted to pH 7.4 was used. PS with radioactive ^{45}Ca (PerkinElmer, Massachusetts, USA) was received by substituting 0.0115 mM of $CaCl_2$ from 1.8 mM$CaCl_2$ with the radioactive one (with 11.2 mCi/l activity). The animals were i/p injected with PS containing ^{40}Ca (named as ^{40}Ca PS) and ^{45}Ca (named as ^{45}Ca PS). The volume of injected solutions was adjusted according to the weight of animals (0.02 ml/g). The ouabain solutions at 10^{-9} M and 10^{-4} M were used for incubation of tissue samples. PS with 50% of NaCl was received by replacing 68.5 mM of NaCl from 137 mM NaCl with 2 M mannitol dissolved in PS for maintaining the osmolarity of the solution. These two types of PS in corresponding figures are named as 100% Na PS and 50% Na PS. All chemicals were obtained from "Medisar" Industrial Chemical Importation Company (Yerevan, Armenia).

2.3. Tissue Preparation

The experimental data were received in *in vivo* and in *in vitro* conditions. The tissue samples from each experiment were investigated after decapitation. Since anesthetics with different chemical and pharmacological profiles have significantly effects on the metabolic processes in tissues [14] [15], in our experiments the animals were sharply immobilized by liquid nitrogen [16] and decapitated. After this procedure full absence of somatic reflexes was recorded. The heart muscle, brain cortex, subcortex and cerebellum tissues were isolated and dissected according to the corresponding experiments.

2.4. Experimental Design

The determination of tissue hydration and Ca uptake was carried out in *in vivo* conditions on young and old rats of intact and i/p injected groups. In each young and old animal groups 3 rats were taken. The animals of intact group were immobilized and decapitated at once and 5 samples from each animal's heart muscle, brain cortex, subcortex and cerebellum tissues were taken. The animals of the next groups were i/p injected with ^{40}Ca PS or ^{45}Ca PS, respectively. After 30 min they were immobilized and decapitated. From each animal, as in case of intact ones, the same number of tissue samples were taken. Thus, from each tissue 15 samples were received, where the water contents and ^{45}Ca uptake were defined. All our experiments were repeated three times.

The comparative effects on tissue hydration after their incubation in ouabain-free and 10^{-9} M, 10^{-4} M ouabain mediums were provided on nine young and old animals in control (preliminarily injected with ^{40}Ca PS) and experimen-

tal (preliminarily injected with ^{45}Ca PS) groups. From each group of animals 45 samples of heart muscle tissue and the same number of brain cortex samples were received. They were divided into 3 parts and incubated separately for 15 min in ouabain free PS (15 samples), 10^{-9} M ouabain solution (15 samples) and 10^{-4} M ouabain solution (15 samples).

The comparative effects on tissue hydration after their incubation in 100% Na PS and 50% Na PS were carried out on two parallel groups of animals. The control group of animals (6 young and 6 old rats) was preliminarily i/p injected with ^{40}Ca PS and from each animal 5 samples of heart muscle and brain cortex tissue were received. After that 15 samples of heart muscle (or brain cortex) tissue were incubated in 100% Na PS for 15 min, while the next 15 samples in 50% Na PS. The identical procedure was repeated on experimental group of young and old animals preliminarily i/p injected with ^{45}Ca PS.

2.5. Definition of Water Content

The water contents of heart muscle, brain cortex, subcortex and cerebellum tissues was determined by traditional "tissue drying" method [17]. After measuring the wet weight (w.w.) of tissue samples they were dried in oven (Factory of Medical Equipment, Odessa, Ukraine) for 24 h at 105˚C for determination of dry weight (d. w.). The quantity of water in 1 g of d.w. tissue was counted by the following equation: (w.w. – d.w.)/d.w.

2.6. Measurement of ^{45}Ca Uptake

The measurement of ^{45}Ca uptake in tissue samples was carried out after the determination of their dry weights. Tissue samples were homogenized in 50 µl of 68% HNO_3 solution. Then 2 ml of Bray's scintillation fluid was added and chemo luminescence of samples were quantified with 1450-MicroBeta liquid scintillation counter (Wallac, Turku, Finland). The quantity of ^{45}Ca in tissue samples was expressed by cpm/mg d. w.

2.7. Statistical Analysis

Microsoft Excel and Sigma-Plot (Version 8.02A, NY, USA) were used for data analyses. The statistical significance in comparison with the control group was calculated with Student's t-test with the following symbols (*$p < 0.05$; **$p < 0.01$; ***$p < 0.001$).

3. Results

Figure 1 shows the results of the experiments where the effects of i/p injections of ^{40}Ca PS and ^{45}Ca PS on tissue hydration are compared with those received from intact animals.

As can be seen, ^{40}Ca PS and ^{45}Ca PS have different effects on heart muscle and brain tissues hydration. The injection of ^{40}Ca PS leads to dehydration in all samples of heart muscle and brain tissues (except in cerebellum tissue of old animals),

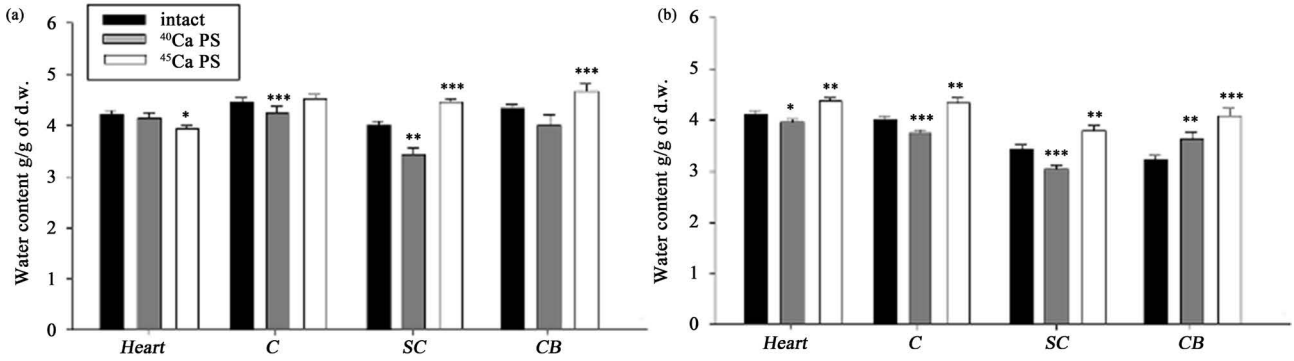

Figure 1. The effects of ^{40}Ca PS and ^{45}Ca PS on hydration of heart muscle (Heart), brain cortex (C), subcortex (SC), cerebellum (CB) tissues of intact and i/p-injected young and old rats. Black bars indicate the mean value of water contents in tissues of intact young (A) and old (b) animals. Gray and white bars indicate the mean value of water contents in tissues of young (a) and old (b) rats injected with ^{40}Ca PS and ^{45}Ca PS, respectively. Each bar represents the mean ± SEM (n = 45). The symbols (*), (**) and (***) indicate $p < 0.05$, $p < 0.01$ and $p < 0.001$, respectively. All data were obtained from three independent experiments.

while the injection of ^{45}Ca PS has dehydration effect on heart muscle tissue of young animals. Meanwhile, in brain tissues of young as well as in heart muscle and brain tissues of old rats the injection of ^{45}Ca PS brings to tissue hydration. Thus, the differences between the effects of ^{40}Ca PS and ^{45}Ca PS on tissue hydration indicate the distinctive nature of hydration mechanisms in heart muscle and brain tissues. In addition, the differences between the effects of ^{40}Ca PS and ^{45}Ca PS in heart muscle and brain cortex tissues have age-dependent increasing character, while in subcortex and cerebellum tissues age-dependent decreasing character was observed (**Figure 1(a)**, **Figure 1(b)**). Our previous study has shown that the high-affinity ouabain receptors (a_3) in the membrane with RNa/Ca exchange function, have more pronounced age-dependent increasing character in brain cortex tissue than in subcortex and cerebellum tissues [9]. Therefore, in the following experiments, brain cortex tissue has been chosen as a subject for the present investigation.

As can be seen in **Figure 2**, the level of ^{45}Ca uptake in heart muscle tissue is much higher than in brain tissues.

However, the age-dependent decrease of ^{45}Ca uptake by brain tissue is more pronounced than in case of heart muscle tissue.

As Ca uptake by RNa/Ca exchange leads to more effective changes of $[Ca]_i$ than by potential-dependent ionic channels [3], we have considered Ca uptake as a result of RNa/^{45}Ca exchange.

It is known that $[Ca]_i$ has multisided effects on intracellular metabolism [18] through which it can cause cell hydration, including the oxidative phosphorylation-induced endogenous water formation [19], the stimulation of Ca-Calmoduline-NO-cGMP pathway-induced activation of Na/Ca exchange in forward (F) mode [11] [20] and inhibition of Na/K-pump activity [21]. Therefore, in the next series of experiments the individual role of each above-mentioned pathway in determination of differences between the effects of $[^{40}Ca]_i$ and $[^{45}Ca]_i$ on heart muscle and brain cortex tissue hydration was studied.

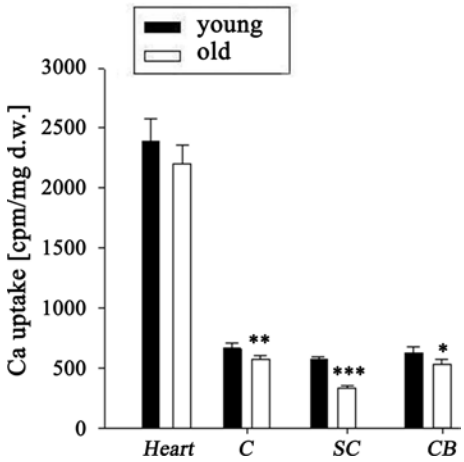

Figure 2. The age-dependent effects of ^{45}Ca uptake in heart muscle (Heart), brain cortex (C), subcortex (SC), cerebellum (CB) tissues. Black and white bars indicate the mean value of ^{45}Ca uptake in tissues of young and old animals, respectively. Each bar represents the mean ± SEM (n = 45). The symbols (*), (**) and (***) indicate $p < 0.05$, $p < 0.01$ and $p < 0.001$, respectively. All data were obtained from three independent experiments.

Considering the high expression of RNa/Ca exchange in heart muscle tissue compared with brain cortex one, it was predicted that in heart muscle tissue the differences between the effects of ^{40}Ca and ^{45}Ca on cell hydration would be more pronounced than in brain tissue. Therefore, to evaluate the nature of the mechanisms through which the effects of ^{40}Ca PS and ^{45}Ca PS on tissues hydration are realized, their effects on tissue hydration in various experimental conditions were studied.

The effects of ^{40}Ca PS and ^{45}Ca PS on heart muscle tissue hydration

The results presented in **Figure 3** show that in ouabain-free PS the hydration of heart muscle samples of young animals injected with ^{40}Ca PS is more pronounced than that of young animals injected with ^{45}Ca PS.

The hydration of heart muscle samples from old animals injected with ^{40}Ca PS is less than the hydration of samples from old animals injected with ^{45}Ca PS (**Figure 3(b)**).

As mentioned in the introduction part of the present study, 10^{-9} M and 10^{-4} M ouabain activate the RNa/Ca exchange by both the decrease of $[Ca]_i$ [7] [11] and the increase of $[Na]_i$ [22], respectively.

The incubation of heart muscle tissue samples of young animals preliminarily injected with ^{40}Ca PS (**Figure 3(a)**) in 10^{-9} M ouabain solution, having cAMP-dependent activation effect on RNa/^{40}Ca exchange [7], causes pronounced dehydration effect, while in heart muscle tissue samples of young animals injected with ^{45}Ca PS, only slight dehydration effect can be recorded. The same study in old animals injected with ^{40}Ca PS shows more pronounced hydration effects as compared with the injection of ^{45}Ca PS (**Figure 3(b)**).

The incubation of heart muscle tissue samples of young animals preliminarily injected with ^{40}Ca PS in 10^{-4} M ouabain solution leads to more pronounced dehydration effect (**Figure 3(a)**) than in case of 10^{-9} M ouabain. However, in heart

muscle tissue samples of young animals injected with ^{45}Ca PS, 10^{-4} M ouabain brings to the same level of dehydration as in the case of 10^{-9} M ouabain (Figure 3(a)).

The same procedures in old animals preliminarily injected with ^{40}Ca PS show that the incubation of their heart muscle tissue samples in 10^{-4} M ouabain leads to the decrease of hydration in contrast to those incubated in 10^{-9} M ouabain (Figure 3(b)). On the other hand, in animals preliminarily injected with ^{45}Ca PS the incubation of heart muscle tissue samples in 10^{-4}M ouabain brings to sharp dehydration (Figure 3(b)). The age-dependent reverse character of hydration, in case when heart muscle tissue samples are incubated in ouabain solutions (compare the continuous lines with the dotted ones in Figure 3(a), Figure 3(b)), is also worth mentioning.

It is known that both 10^{-9} M and 10^{-4} M ouabain-induced activations of RNa/Ca exchange are accompanied with the increase of intracellular cAMP contents [12], having an important role in muscle contractility (hydration). Therefore, to exclude the role of cAMP contents in determination of differences between the effects of activation of RNa/^{40}Ca and RNa/^{45}Ca exchange on heart muscle tissue hydration, in the next series of experiments the mentioned differences are studied by the decrease of Na gradient on the membrane. For this purpose, two various ages of animals were preliminarily injected with ^{40}Na PS (^{40}Ca or with ^{45}Ca) and 30 min later their heart muscle tissue samples were separately incubated in 100% Na PS and 50% Na PS.

As can be seen in Figure 4, the decrease of Na ions ($[Na]_o$) concentration by 50% in cell bathing medium leads to more pronounced dehydration in heart

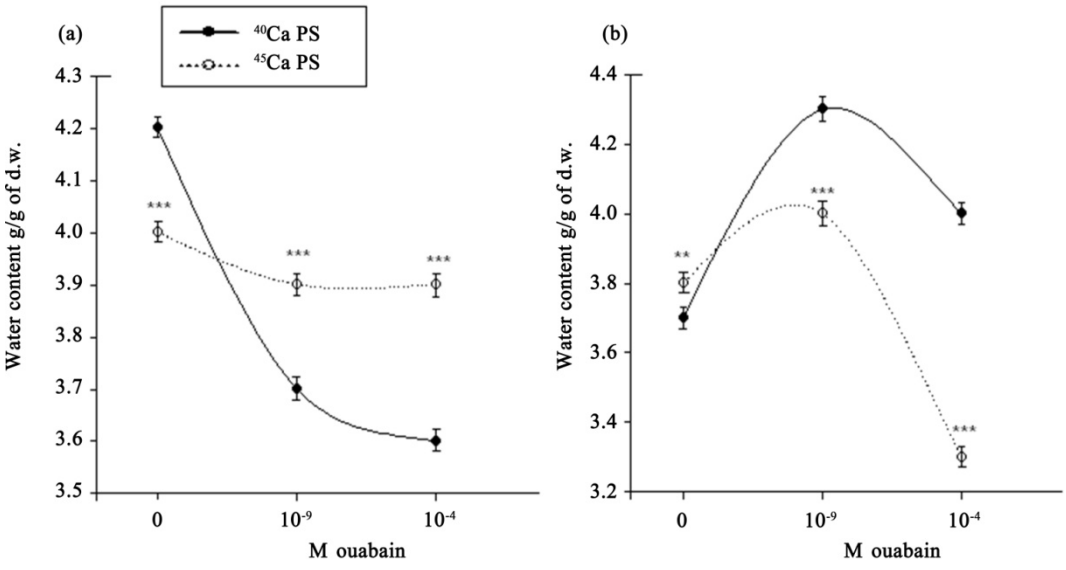

Figure 3. The effects of ouabain-free PS, 10^{-9} M and 10^{-4} M ouabain solutions on water contents variation in heart muscle tissue samples of young (a) and old (b) animals preliminarily injected with ^{40}Ca PS (continuous lines) and ^{45}Ca PS (dotted lines). Each point in line represents the mean ± SEM (n = 45). The symbols (**) and (***) indicate $p < 0.01$ and $p < 0.001$, respectively. All data were obtained from three independent experiments.

muscle tissue samples than in heart muscle tissue samples incubated in normal 100% Na PS.

However, the dehydration effect induced by 50% Na PS is more expressed in heart muscle tissue samples of animals injected with ^{45}Ca PS than in those injected with ^{40}Ca PS (Figure 4(a), Figure 4(b)).

The effects of ^{40}Ca PS and ^{45}Ca PS on brain cortex tissue hydration

The same protocols of experiments performed on heart muscle tissue were repeated with brain cortex tissue. The data presented in Figure 5 indicate that in ouabain-free PS brain cortex tissue samples of young as well as of old animals preliminarily injected with ^{40}Ca in ouabain-free PS are more dehydrated than those animals injected with ^{45}Ca, while the incubation of brain cortex tissue samples of young rats injected with ^{40}Ca in 10^{-9} M ouabain shows significantly higher level of hydration as compared with the samples of animals injected with ^{45}Ca (Figure 5(a)).

The incubation of brain cortex tissue samples of young rats injected with ^{40}Ca PS in 10^{-4} M ouabain leads to dehydration, while the same procedure in young rats injected with ^{45}Ca appears to have less pronounced hydration effect: *i.e.* there is a slight dose-dependent increase of tissue hydration at ouabain (Figure 5(a)).

As can be seen in Figure 5(b), the incubation of brain cortex tissue samples of old animals preliminarily injected with ^{40}Ca PS in 10^{-9} M and 10^{-4} M ouabain medium brings to dose-dependent increase of hydration level, while in case of old animals injected with ^{45}Ca PS brain cortex tissue hydration is slightly increased in 10^{-9} M ouabain and decreased in 10^{-4} M ouabain medium.

The effects of 100% Na PS and 50% Na PS on brain cortex tissue hydration are

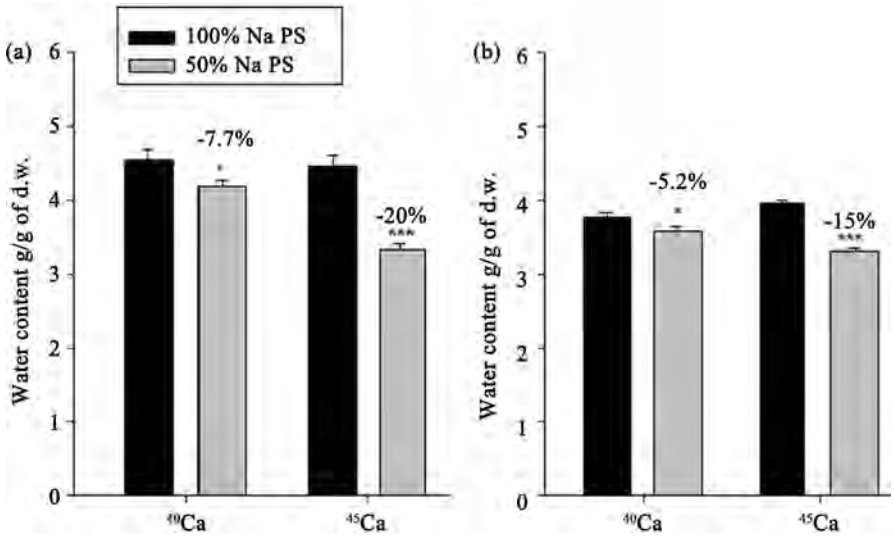

Figure 4. The effects of 100% Na PS (black bars) and 50% Na PS (white bars) on water contents variation in heart muscle tissue samples of young (a) and old (b) rats preliminary injected with ^{40}Ca PS and ^{45}Ca PS. The numbers in % indicate the difference between levels of hydration. Each bar represents the mean ± SEM (n = 45). The symbols (*) and (***) indicate $p < 0.05$ and $p < 0.001$, respectively. All data were obtained from three independent experiments.

the same as in the identical case of heart muscle tissue hydration (Figure 4). As is shown in Figure 6(a), Figure 6(b).

The dehydration in brain cortex tissue samples incubated in 50% Na PS is more pronounced in animals of both ages, which are preliminarily injected with ^{45}Ca PS, than in tissue samples of animals preliminarily injected with ^{40}Ca PS.

4. Discussion

It is known that Ca uptake by cells is realized by potential-dependent ionic channels and RNa/Ca exchange. As the threshold of RNa/Ca exchange activation

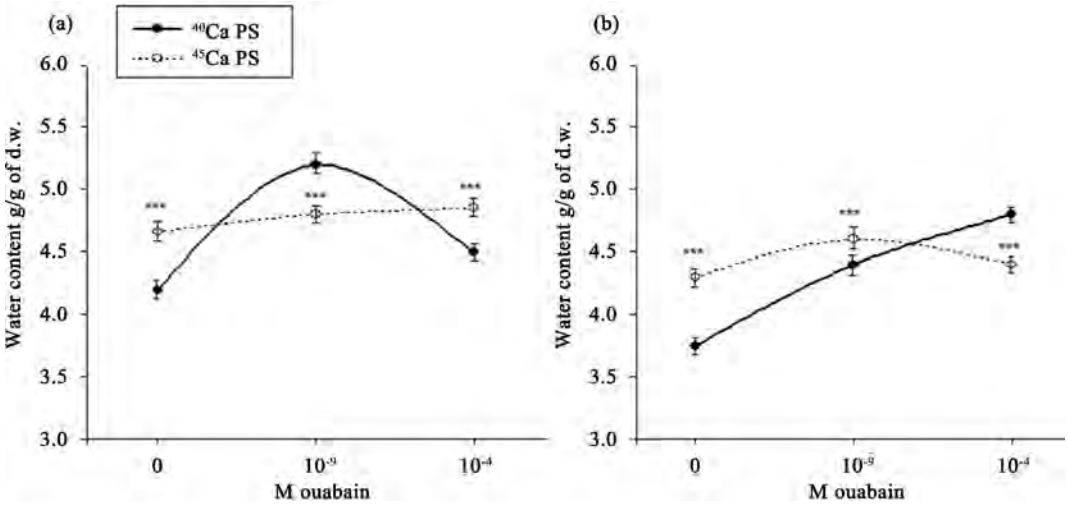

Figure 5. The effects of ouabain-free PS, 10^{-9} M and 10^{-4} M ouabain solutions on water content variation in brain cortex tissue samples of young (a) and old (b) animals preliminary injected with ^{40}Ca PS (continuous lines) and ^{45}Ca PS (dotted lines). Each point in line represents the mean ± SEM (n = 45). The symbol (***) indicate $p < 0.001$, respectively. All data were obtained from three independent experiments.

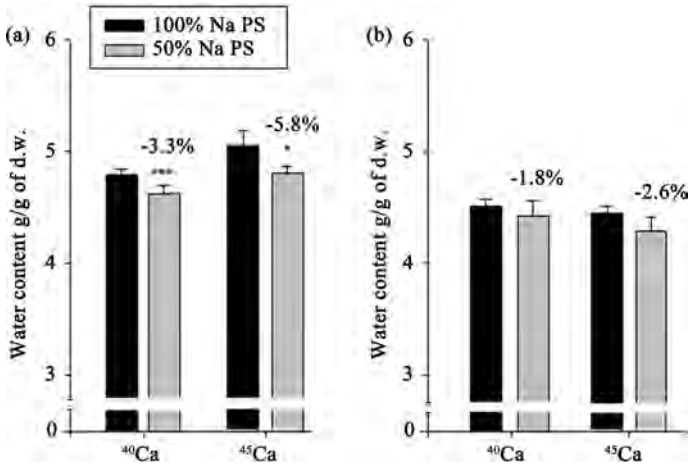

Figure 6. The effects of 100% Na PS (black bars) and 50% Na PS (white bars) on water contents variation in brain cortex tissue samples of young (a) and old (b) rats preliminarily injected with ^{40}Ca PS and ^{45}Ca PS. The numbers in % indicate the difference between levels of hydration. Each bar represents the mean ± SEM (n = 45). The symbols (*) and (***) indicate $p < 0.05$ and $p < 0.001$, respectively. All data were obtained from three independent experiments.

is incomparable less than of ionic channel activity, in the present experiments, the PS injection-induced stimulation of Ca uptake can mainly be considered as a result of RNa/Ca exchange activation [3]. As the energy source for RNa/Ca exchange is E_{ca} - E_{Na}, it is predicted that $E_{45Ca} > E_{40Ca,}$ because of $[^{45}Ca]_i$, is close to "0" mM. Therefore, it is predicted that the rate of RNa/^{45}Ca exchange must be higher than the rate of RNa/^{40}Ca exchange. However, it is not clear whether the physiological difference between the activations of RNa/^{40}Ca and RNa/^{45}Ca exchange is only due to their different rates or not.

As was noted in introduction part, the activation of RNa/Ca exchange has double effects on cell hydration: passive-dehydration because of its electrogenic character and $[Ca]_i$-induced metabolic effects. The obtained data showing that the activation of RNa/^{40}Ca and RNa/^{45}Ca exchanges has different effects on heart muscle and brain tissue hydration with age-dependent character reveals the different metabolic effects of intracellular $[^{40}Ca]_i$ and $[^{45}Ca]_i$ on cell hydration (**Figure 1**).

By previous study it has been shown that the increase of $[Ca]_i$ leads to heart muscle hydration because of activation of Ca-Calmoduline-NO-cGMP-induced stimulation of FNa/Ca exchange [22]. The data that in young rats the activation of RNa/^{45}Ca exchange has more pronounced dehydration effect than the activation of RNa/^{40}Ca exchange, and in heart muscle tissue of old rats it leads to more hydration compared with the activation of RNa/^{40}Ca exchange in ouabain-free medium, can support the suggestion that the rate of RNa/^{45}Ca exchange is higher than the rate of RNa/^{40}Ca exchange. The RNa/^{45}Ca exchange-induced brain tissue hydration compared with the activation of RNa/^{40}Ca exchange (**Figure 1(a)** and **Figure 1(b)**) can be explained by the same mechanism.

The data on age-dependent decrease of ^{45}Ca uptake by tissues can be considered as a result of aging-induced increase of $[Ca]_i$, which is in harmony with literature data [2]. It is worth noting that in spite of the fact that the expression of RNa/Ca exchange in heart muscle tissue is much higher than in brain tissue, the age-dependent decrease of Ca uptake in brain tissue is more pronounced than in heart muscle tissues (**Figure 2**). Such a weak age-dependency of Ca uptake in heart muscle tissue probably can be explained by higher $[Ca]_i$-buffering properties of heart muscle tissue as compared with brain tissue. Therefore, we suggest that discussing the comparative results of the effects of ^{40}Ca PS and ^{45}Ca PS on heart muscle and brain tissues could help to evaluate the nature of different metabolic mechanisms of $[^{40}Ca]_i$ and $[^{45}Ca]_i$.

The effects of ^{40}Ca PS and ^{45}Ca PS on heart muscle tissue hydration

The obtained data that in ouabain-free medium heart muscle tissue samples from young and old rats injected with ^{45}Ca PS are dehydrated and hydrated, respectively, compared with heart muscle hydration of animals injected with ^{40}Ca PS (**Figure 3(a)**, **Figure 3(b)**), can be explained by the above mentioned suggestion that the rate of RNa/^{45}Ca exchange is higher than the rate of RNa/^{40}Ca exchange. The results showing that heart muscle tissue samples of ^{40}Ca PS-injected

young rats are sharply dehydrated upon the impact of 10^{-9} M and 10^{-4} M ouabain, while in the rats injected with ^{45}Ca PS both concentrations of ouabain have slight dehydration effects on muscle (**Figure 3(a)**), can probably be explained by ^{45}Ca-induced transition of cytoplasm from sol into gel state because of high Ca-dependent phosphorylation of myofibrils in cytosol or by compensation of RNa/^{45}Ca exchange-induced dehydration by hydration of FNa/Ca exchange activation in result of high $[^{45}Ca]_i$-induced activation of Ca-Calmoduline-NO-cGMP pathway [11].

The obtained result that in old rats injected with ^{45}Ca PS heart muscle tissue hydration becomes ouabain-sensitive is probably due to age-dependent weakening of heart muscle contractility leading to abnormal increase of $[Ca]_i$ as well as aging-induced dysfunction of intracellular cAMP controlling system.

The 10^{-9} M ouabain-activation of RNa/Ca exchange which leads to heart muscle hydration can be explained by $[Ca]_i$-induced activation of mitochondrial function leading to stimulation of endogenous water molecules' formation, which is based on our previous data [19]. The fact that the 10^{-9} M ouabain-induced activation of RNa/^{45}Ca exchange has less pronounced hydration effects on heart muscle of young animals than the activation of RNa/^{40}Ca exchange (**Figure 3**) can also be explained by high $[^{45}Ca]_i$ leading to depression of 10^{-9} M induced activation of RNa/Ca exchange.

The strong dehydration effect of RNa/^{45}Ca exchange at 10^{-4} M ouabain in heart muscle of old animals supports the previous suggestion that the dehydration effect of RNa/^{45}Ca exchange on heart muscle becomes more effective at high $[Na]_i$, when Na/K pump is in inactive state.

The effect of ^{45}Ca-induced stabilization of muscle hydration in young rats and its absence in aged ones seems extremely interesting and the elucidation of its exact mechanism can serve as a subject for a special investigation.

The data revealing that 50% Na PS-induced activation of RNa/^{45}Ca exchange has stronger effects on muscle hydration than RNa/^{40}Caexchange activation (**Figure 4**) indicate that the rate of RNa/^{45}Ca exchange is higher than that rate of RNa/^{40}Ca exchange.

The effects of R Na/^{40}Ca and R Na/^{45}Ca exchange on brain cortex tissue hydration

As in the case of heart muscle study, the data showing that in ouabain-free PS brain cortex tissue samples of young as well as of old animals preliminarily injected with ^{40}Ca are more dehydrated than of those of animals injected with ^{45}Ca PS (**Figure 5**) can be explained by high rate of RNa/^{45}Ca exchange compared with rate of RNa/^{40}Ca exchange. The RNa/^{45}Ca exchange brings to hydration through elevation of $[^{45}Ca]_i$ than by activation of FNa/Ca exchange and passive dehydration effect on tissue, respectively. The data that in 10^{-9} M ouabain brain cortex tissue samples of young animals injected with ^{40}Ca PS demonstrate hydration effect through $[Ca]_i$-induced increase of endogenous water formation by mitochondria [19] and in the same conditions the absence of such effect in

young animals injected with ^{45}Ca PS and less sensitivity to 10^{-4} M ouabain (**Figure 5(a)**) allow us to suggest that $[^{45}Ca]_{i,}$ besides the activation of FNa/Ca exchange, which can balance RNa/Ca exchange-induced tissue dehydration by an unknown mechanism, also causes transformation of cytoplasm from sol into gel state in young animals. The data that in 10^{-9} M and 10^{-4} M ouabain mediums the hydration level of brain cortex samples from ^{40}Ca PS-injected old rats has dose-dependent increasing character, while in the case of ^{45}CaPS-injected animals brain cortex tissue hydration is slightly increased in 10^{-9} M ouabain and decreased in 10^{-4} M ouabain mediums indicate that $[^{45}Ca]_i$-induced stabilizing mechanism of brain cortex hydration in young animals has age-dependent weakening character.

The data that in both ages of animals the decrease of $[Na]_o$ leads to more pronounced dehydration in cortex samples of ^{45}Ca PS-injected animals compared to dehydration in cortex samples from ^{40}Ca PS-injected animals can be an additional support for the aforementioned suggestion that the rate of RNa/^{45}Ca exchange is higher than the rate of RNa/^{40}Ca exchange (6A and B).

5. Conclusions

Thus, the obtained data of the present work bring us to the following conclusions:

- The intraperitoneal injections of ^{40}Ca PS and ^{45}Ca PS which bring to activation of RNa/^{40}Ca and RNa/^{45}Ca exchange, respectively, have different effects on heart muscle and brain tissue hydration with different age-dependent characters.
- These differences between RNa/^{40}Ca and RNa/^{45}Ca exchange-induced tissue hydrations are much more pronounced in heart muscle tissues than in brain tissues as RNa/Ca exchange is expressed incomparably higher in heart muscle tissues than in brain tissues.
- The rate of RNa/^{45}Ca exchange is higher than the rate of RNa/^{40}Ca exchange, because of $E_{45Ca} > E_{40Ca}$.
- The $[^{45}Ca]_i$ and $[^{40}Ca]_i$ have different metabolic effects on heart muscle and brain cortex tissue hydration. In young animals tissue hydration in the case of $[^{40}Ca]_i$ has dose-dependent ouabain sensitivity, while in the case of $[^{45}Ca]_i$ tissue hydration becomes ouabain-insensitive. Upon the impact of $[^{45}Ca]_i$, the heart muscle tissue hydration of old rats becomes ouabain-sensitive, while brain cortex tissue hydration remains significantly less ouabain-sensitive than in the case of $[^{40}Ca]_i$.
- The main summary of this work is that radioactive ^{45}Ca is not bioequivalent to cold ^{40}Ca. Therefore, ^{45}Ca cannot be used in biological experiments for evaluation of the functional role of ^{40}Ca.

Acknowledgements

We express our gratitude to Ani Gyurjinyan from UNESCO Chair in Life

Sciences for editorial work.

Conflicts of Interest

The authors declare no conflicts of interest regarding the publication of this paper.

References

[1] Ayrapetyan, S.N., Rychkov, G.Y. and Suleymanyan, M.A. (1988) Effects of Water Flow on Transmembrane Ionic Currents in Neurons of *Helix pomatia* and in Squid Giant Axon. *Comparative Biochemistry and Physiology Part A*, **89**, 179-186. https://doi.org/10.1016/0300-9629(88)91076-6

[2] Khachaturian, Z.S. (1989) The Role of Calcium Regulation in Brain Aging: Reexamination of a Hypothesis. *Aging Clinical and Experimental Research*, **1**, 17-34. https://doi.org/10.1007/BF03323872

[3] Blaustein, N.P. and Lederer, W.J. (1999) Na^+/Ca^{2+} Exchange. Its Physiological Implications. *Physiological Reviews*, **79**, 763-854. https://doi.org/10.1152/physrev.1999.79.3.763

[4] Ayrapetyan, S.N., Suleymanyan, M.A., Saghyan, A.A. and Dadalyan, S.S. (1984) Autoregulation of Electrogenic Sodium Pump. *Cellular and Molecular Neurobiology*, **4**, 367-383. https://doi.org/10.1007/BF00733598

[5] Dadalyan, S.S., Azatian, K.V. and Ayrapetyan, S.N. (1988) On the Effect of Low Concentrations of Neurotransmitters in Sodium Efflux and Cyclic Nucleotides Level in Snail Neurons. *Neurochemistry*, **7**, 18-25. (In Russian)

[6] Ayrapetyan, S.N. and Carpenter, D.O. (1991). Very Low Concentrations of Acetylcholine and GABA Modulate Transmitter Responses. *NeuroReport*, **2**, 563-565. https://doi.org/10.1097/00001756-199110000-00002

[7] Sagian, A.A., Ayrapetyan, S.N. and Carpenter, D.O. (1996) Low Concentrations of Ouabain Stimulate Na:Ca Exchange in Neurons. *Cellular and Molecular Neurobiology*, **16**, 489-498. https://doi.org/10.1007/BF02150229

[8] Ayrapetyan, G.S., Papanyan, A.V., Hayrapetyan, H.V. and Ayrapetyan, S.N. (2005) Metabolic Pathway of Magnetized Fluid-Induced Relaxation Effects on Heart Muscle. *Bioelectromagnetics*, **26**, 624-630. https://doi.org/10.1002/bem.20145

[9] Ayrapetyan, S., Heqimyan, A. and Nikoghosyan, A. (2012) Age-Dependent Brain Tissue Hydration, Ca Exchange and Their Dose-Dependent Ouabain Sensitivity. *Journal of Bioequivalence & Bioavailability*, **4**, 60-68. https://doi.org/10.4172/jbb.10000114

[10] Heqimyan, A., Narinyan, L., Nikoghosyan, A., *et al.* (2012) Age-Dependency of High Affinity Ouabain Receptors and Their Magnetosensitivity. *The Environmentalist*, **32**, 228-235. https://doi.org/10.1007/s10669-011-9383-0

[11] Brini, M. and Carafoli, E. (2009) Calcium Pumps in Health and Disease. *Physiological Reviews*, **89**, 1341-1378. https://doi.org/10.1152/physrev.00032.2008

[12] Ayrapetyan, S., Carpenter, D., Saghyan, A.A., Dadalian, S., Martirosyan, D. and Mndalian, V. (1992) Extralowneutotransmitter Doses-Induced Triggering of Neuronal Intracellular Messenger Systems. In: Kostyuk, P. and Ostrowskii, M., Eds., *Cellular Signalization*, Nauka, Moscow, 89-96.

[13] Nikoghosyan, A., Narinyan, L., Heqimyan, A. and Ayrapetyan, S. (2018) The Quantum-Mechanical Sensitivity of Cell Hydration in Mammals. *Open Journal of*

Biophysics, **8**, 104-116. https://doi.org/10.4236/ojbiphy.2018.83009

[14] Heqimyan, A., Deghoyan, A. and Ayrapetyan, S. (2011) Ketamine-Induced Cell Dehydration as a Mechanism of Its Analgesic and Anesthetic Effects. *Journal of International Dental and Medical Research*, **4**, 42-49.

[15] Takahashi, R. and Aprison, M. (1964) Acetylcholine Content of Discrete Areas of the Brain Obtained by a Near-Freezing Method. *Journal of Neurochemistry*, **11**, 887-892. https://doi.org/10.1111/j.1471-4159.1964.tb06740.x

[16] Adrian, R.H. (1956) The Effect of Internal and External Potassium Concentration on the Membrane Potential of Frog Muscle. *Journal of Physiology*, **133**, 631-658. https://doi.org/10.1113/jphysiol.1956.sp005615

[17] Carafoli, E. (1994) Biogenesis: Plasma Membrane Calcium ATPase: 15 Years of Work on the Purified Enzyme. *FASEB Journal*, **8**, 993-1002. https://doi.org/10.1096/fasebj.8.13.7926378

[18] Lehninger, A.L. (1970) Mitochondria and Calcium Ion Transport. *Biochemical Journal*, **119**, 129-138. https://doi.org/10.1042/bj1190129

[19] Azatian, K.V., White, A.R., Walker, R.J. and Ayrapetyan, S.N. (1998) Cellular and Molecular Mechanisms of Nitric Oxide-Induced Heart Muscle Relaxation. *General Pharmacology*, **30**, 543-553. https://doi.org/10.1016/S0306-3623(97)00302-9

[20] Skou, J. (1957) The Influence of Some Cations on an Adenosine Triphosphatase from Peripheral Nerves. *Biochimica et Biophysica Acta*, **23**, 394-401. https://doi.org/10.1016/0006-3002(57)90343-8

[21] Baker, P.F., Blaustein, M.P., Hodgkin, A.L. and Steinhardt, S.A. (1969) The Influence of Calcium on Sodium Efflux in Squid Axons. *The Journal of Physiology*, **200**, 431-458. https://doi.org/10.1113/jphysiol.1969.sp008702

[22] Narinyan, L.Y., Ayrapetyan, G.S., De, J. and Ayrapetyan, S.N. (2014) Age-Dependent Increase in Ca^{2+} Exchange Magnetosensitivity in Rat Heart Muscles. *Biochemistry and Biophysics*, **2**, 39-49.

Scientific Research Publishing

Open Journal of Biophysics, 2020, 10, 27-45
https://www.scirp.org/journal/ojbiphy
ISSN Online: 2164-5396
ISSN Print: 2164-5388

Electrostatic Contributions to Carcinogenesis

L. John Gagliardi[1], Daniel H. Shain[2*]

[1]Departments of Physics, Rutgers The State University of New Jersey, Camden, NJ, USA
[2]Departments of Biology, Rutgers The State University of New Jersey, Camden, NJ, USA
Email: gagliard@scarletmail.rutgers.edu, *dshain@camden.rutgers.edu

How to cite this paper: Gagliardi, L.J. and Shain, D.H. (2020) Electrostatic Contributions to Carcinogenesis. *Open Journal of Biophysics*, **10**, 27-45.
https://doi.org/10.4236/ojbiphy.2020.101003

Received: November 29, 2019
Accepted: January 13, 2020
Published: January 16, 2020

Abstract

Nanoscale electrostatics plays important roles in aster (spindle) assembly and motion, nuclear envelope breakdown and reassembly, and in force generation at kinetochores, poles, and chromosome arms for prometaphase, metaphase, and anaphase—A chromosome motions during mitosis. A large body of experimental evidence also suggests a role for electrostatics as the trigger for mitosis, which is considered here particularly in the context of cancer. Cancer cells are characterized by impaired intercellular electrical communication and adhesive contact as well as a loss of contact inhibition, conditions associated with increased cell surface negativity relative to their normal counterparts. Dividing cells have also been associated with lower transmembrane potentials and altered intracellular ionic concentrations. Here we propose that cancer cells are distinguished by abnormal trans- and intramembrane electric potentials, leading to the loss of active Na+/K+ plasma membrane pumping, increased intracellular concentrations of sodium and other ions, and alkaline nucleo-cytoplasmic pH, all of which are associated with and integral to carcinogenesis.

Keywords

Division, Malignant, Mitosis, Cancer, Alkalinity

1. Introduction

The electromagnetic interaction is primarily responsible for the structure of matter from atoms to objects. Much of physics, all of chemistry, and most of biology are in this size realm. Primitive eukaryotic cells had to divide prior to the evolution of many biological mechanisms, and it is reasonable to assume that electrostatics, a component of the electromagnetic interaction, played (and continues to play), an important role in the mechanics of chromosome motions during mitosis [1] [2] [3] [4] [5].

The cancer problem is characterized by the existence of cells that divide when they should not. An explanation of this behavior has emerged as one of the signature problems in biology. With an abundance of proposals regarding the trigger for cancerous cell division, how does one decide which approach is the most compelling? Regarding scientific models, the renowned physicist Paul Ehrenfest suggested that they should be framed in such a manner that "the essence lies in recognizing the connections in all directions." Recognizing a number of connections between increased cancer cell surface negativity motivated Van Beek *et al.* [6] to suggest some time ago that increased cell surface membrane-bound negative charge is a general feature of cancer cells.

Mammalian cells are known to have bound negative charges on their surfaces. This surface charge density σ C/m^2 (Coulombs per square meter) is due largely to ionized carboxyl groups of sialic acid residues [7] [8] [9]. Net surface negativity is primarily a function of the density of these anionic groups anchored in the membrane at the cell surface, but it also depends on the pH and ionic strength of the surrounding medium [10]. Other acidic groups may reside at the cell surface [11], and some cells have anionic groups associated with RNA at their periphery [12].

Studies on cells transformed by oncogenic viruses suggest that the altered growth pattern of these cells is caused by changes at the cell surface [13]. Importantly, changes at the cell surface often involve the carbohydrate components of glycolipids and glycoproteins, including an increase of fucose-labeled glycoprotein with increased sialic acid density [6] [11] [14] [15]. Quite some time ago, it was proposed that increased sialic acid density at the surfaces of transformed and malignant cells could be a general characteristic of cancer cells [6].

It is well established that transformed and malignant cells suffer from drastically impaired intercellular communication [16]. One of the most well known characteristics of cancer cells is that, unlike normal cells, they do not stop dividing upon functional cellular contact (*i.e.*, cellular contact that leads to the expression of a signal inhibitory to S-phase initiation). Studies on a variety of mature cell types *in vivo* have shown that the great majority are arrested in the G_1 period of the cell cycle [17], and must pass through the S period of DNA synthesis before entering mitosis, although a small fraction may be arrested in the G_2 period [18].

A number of studies have demonstrated the importance of sialic acid [11] [19] [20]-[25] and other cell surface carbohydrates [11] [26] in cell contact and recognition phenomena. In principle, increased density of sialic acid could prevent the intimate association necessary to establish intercellular contact, either directly due to the increased charge, or indirectly by masking other carbohydrate residues involved in functional contact.

Another long-standing set of observations concerns differences between the transmembrane electric potential of cycling (*i.e.*, dividing) and non-cycling cells [27] [28] [29] [30]. These studies have shown that the former have much lower

transmembrane potentials and different intracellular concentrations of inorganic ions (henceforth simply designated "ions"). An example of a significant decrease in transmembrane potential ΔV_m is observed in cellular adaptation from *in vivo* non-dividing conditions to growth (dividing cells) *in vitro*. Thus the interphase (G_1) ΔV_m level of −50 to −60 mV for typical mature somatic cells *in vivo* undergoes a change to *in vitro* G_1 levels in the vicinity of −10 mV. This well-known decrease appears to be a general phenomenon. Also noteworthy is the pronounced membrane *depolarization* (approx. −90 mV to −10 mV) accompanying malignant transformation of somatic cells *in vivo* [31] [32] [33].

We propose here that electrostatics was, and currently remains, integral to the initiation of cell division (*i.e.*, mitogenesis). Moreover, differences in ion concentrations and overall ionic strength are both important aspects of the disparity in measured transmembrane potentials of dividing versus non-dividing cells, as considered below.

2. Mechanical Equilibrium of a Membrane

The mechanical equilibrium of a model half-membrane is depicted schematically in Figure 1. The hemispherical shell, representing half of the membrane, is in equilibrium under the action of a uniform surface tension acting in the $-x$ direction from the rest of the membrane, and surface forces acting perpendicularly outward from the surface everywhere over the hemisphere. The surface forces arise from both the pressure difference across the membrane and a surface electrical force per unit area of the membrane (*i.e.*, membrane electrostatic stress). These forces may be envisaged if one considers a charged balloon in equilibrium under 1) the surface tension forces due to the elastic deformation of the rubber, 2) the pressure difference between the inside and outside of the balloon, and 3) a membrane electrostatic stress (ES) due to the mutual repulsion of like negative

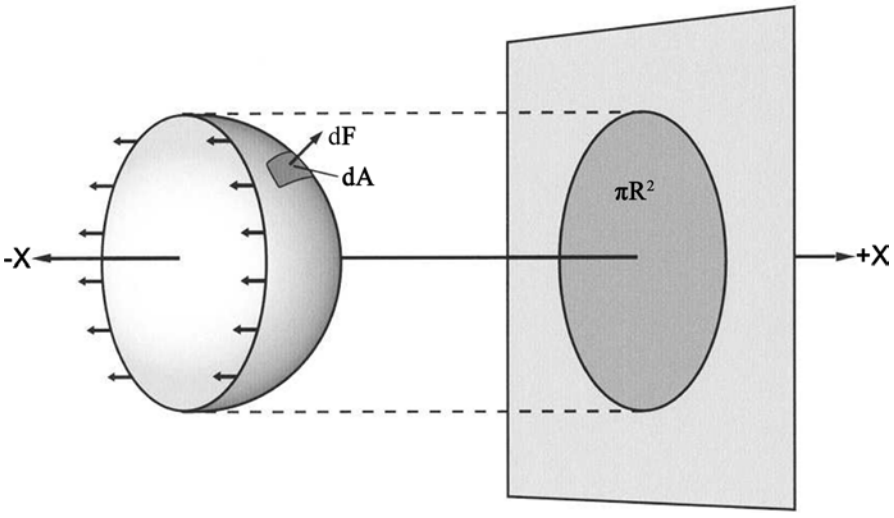

Figure 1. Model half-membrane in equilibrium. The spherical half-membrane is in equilibrium under membrane surface tension forces acting to the left and electrical stress plus hydrostatic force components acting to the right.

charges fixed to the surface. The use of a spherical shell is clearly an idealization; however, the analysis presented here is valid for a large class of ellipsoids of revolution, with the mathematics being far simpler for a spherical geometry.

The differential electrostatic force $\mathrm{d}F_e$ acting perpendicularly to an element of area $\mathrm{d}A$ of a charged surface can be expressed by the following equation [34].

$$\mathrm{d}F_e = \left(\varepsilon E^2/2\right)\mathrm{d}A = \left(\sigma^2/2\varepsilon\right)\mathrm{d}A \tag{1}$$

where E^2 is the magnitude squared of the electric field at $\mathrm{d}A$, ε is the local permittivity just outside the surface at $\mathrm{d}A$, and σ is the net surface charge per unit area. The half-membrane will be in equilibrium if the surface tension element of force, $\gamma \mathrm{d}l$ (where γ is the membrane surface tension in N/m) integrated around the circumference of the membrane ($2\pi R\ \gamma$), is equal to the total force in the $+x$ direction. Integrating the component in the $+x$ direction of the total differential force $\mathrm{d}F$, which arises from ES plus the pressure difference ($p_1 - p_2$) across the membranes, we find that

$$2\gamma/R = \Delta p + \sigma^2/2\varepsilon \tag{2}$$

where $\Delta p = (p_1 - p_2)$, where p_1 is the pressure inside. This equation governs the equilibrium of the model half-membrane.

Studies have shown that ES manifests itself in membrane equilibrium. After a series of experiments on cell deformability, Weiss [35] concluded that terminal sialic acids contribute to the mechanical properties of the cell periphery through electrostatic repulsion between their own and other anionic groups. Cells in this study became more deformable after incubation with neuraminidase, an enzyme which removes negatively charged sialic acid residues from the cell surface. In animal cells, the terminal sialic acids are attached to cell (plasma) membrane proteins, which are firmly anchored in the lipid bilayer. Therefore, it is reasonable to assume that the repulsive interactions between these groups are primarily responsible for the observed decrease in the deformability of cells with more surface negative charge.

If Δp were larger than $\sigma^2/2\varepsilon$, removal of a significant portion of surface charge by treatment with neuraminidase would not be consistent with the observed increase in the deformability of these cells [35]. We may therefore assume that the Δp term is at most comparable in magnitude to the $\sigma^2/2\varepsilon$ contribution to membrane stress. Accordingly, it is possible to obtain a good approximation for the equilibrium of a membrane from (2) written as:

$$\sigma^2/2\varepsilon \approx 2\gamma/R \tag{3}$$

It is well established in electrochemistry [36] that the permittivity of the first few water layers outside a charged surface is an order of magnitude smaller than that of the bulk phase. The effective permittivity of water as a function of distance from a charged surface has been determined by atomic force microscopy [37] to increase monotonically from 4 - 6 ε_0 at the interface to 78 ε_0 at a distance of 25 nm from the interface. The values of dielectric constants $k(x)$ at distances of 1, 2, 3 and 4 nm from a charged surface were measured to be 9, 21, 40 and 60,

respectively. The value of ε at the membrane outer (cytoplasmic) surface may therefore be conservatively estimated as 30 ε_0, where ε_0 is the permittivity of free space, 8.85 pF/m (picoFarads/meter). The experiment was carried out with mica, which has a surface charge density that varies from 1 to 50 mC/m^2, in the same range as biological surfaces [38] [39].

The range for γ may be taken as 0.1 to 1.0 dyne/cm (0.1 to 1 mN/m) [40]. These values, when substituted into (3), using R = 20 μm and ε = 30 ε_0 = 270 pF/m (picoFarads/meter), give a range of values for σ from 73 to 230 μC/m^2 (microCoulombs/square meter). Values of σ in this range are sufficient to exert an electrostatic stress comparable to $2\gamma/R$ in the cell membrane. Experimental values for the surface charge density of biological and artificial lipid membranes range from 0.4 to 160 mC/m^2 (milliCoulombs/square meter) [38] [39] [41] [42]. This calculation strongly suggests that electrostatic stress is an important factor in the equilibrium and thermodynamics of the plasma membrane.

Cell electrophoresis studies have identified a 12% - 18% increase in plasma membrane negativity just prior to cell division [43] [44], consistent with an observed increase of 50% in the whole cell content of sialic acid during mitosis [45]. Importantly, note that

$$\Delta\left(\sigma^2\right)/\sigma^2 \approx 2\Delta\sigma/\sigma \tag{4}$$

and an increase of 15% in cell membrane negativity corresponds to a 30% increase in cell surface electrostatic stress. Similar increases may be expected for the membranes of the nuclear envelope [2] and mitochondria.

Increased ES on the plasma membrane could explain the well-known observation that cells typically assume a more spherical shape (*i.e.*, "round out") during cell division. As referenced above, an increased density of sialic acid in the surface glycoproteins of transformed and malignant cells has been observed in a number of studies. This is consistent with the common observation that cancer cells are characteristically rounded and "puffy" in appearance, possibly from permanently increased ES on these cells.

A number of experimental studies have revealed that the plasma membrane transport properties of transformed cells differ from their normal counterparts [46]. As indicated above, an increased membrane charge density, with its associated increase in ES, is large enough to be manifested in the equilibrium of cellular membranes. Increased ES, along with other factors, could therefore be related to the observed altered transport properties of the plasma membrane (see below).

Elevated surface charge may also interfere with the formation of gap junctions, which provide an important mechanism for coordinating the activities of neighboring cells. These specialized cell-cell junctions form between closely apposed cell membranes to directly connect the cytosols of the joined cells with narrow canals through which small molecules and ions can pass. A number of studies have shown that embryonic cells make and break gap junction connections in definite patterns, suggesting they play a role in coordinating cell division

and growth [29] [47]. It therefore seems likely that the greatly increased intercellular electrical resistance of abnormal cells [16] is due to defective or reduced numbers of gap junctions, and that increased sialyl extension [6] from the greater surface charge density is at least partially responsible for this condition.

Thus abnormal cells exhibit a greatly increased intercellular electrical resistance, indicative of abnormal barriers to the flow of ions between cells. The greater surface charge exhibited by cancer cells has been associated with defective cell-cell contacts, likely a major contributing factor to the inability of cancer cells to form normal gap junctions. Because intercellular communication via properly functioning gap junctions is necessary, maintenance of non-mitogenic intracellular ionic concentrations over organ-size volumes may operate as a *social* control over cell division that is utilized by multicellular organisms (see below). This could be one possible explanation for the existence of local pockets of cancer cells—presumably with defective gap junctions and a resulting defective intercellular communication—within organs surrounded by normal cells, a common observation in tumor histology.

As noted, numerous observations regarding cancer cells have revealed that sialic acid is involved in cell contact [19] [23] [24] [26] [48] [49] [50] and growth control by functional contact [51] [52] [53]. For these and other reasons, an increased density of membrane-bound, negatively charged sialic acid at the cancer cell surface has been suggested as a general characteristic of malignant cells [6]. In the context of electrostatics, these experimental observations underlie the primary conditions that regulate mitogenesis. In particular, we propose that increased cell surface charge significantly influences the intramembrane electric potential, with implications for the active transport of ions as well as the operation of ion channels, as detailed below.

3. Membrane Electric Potentials and Intracellular Ionic Concentrations

Membrane potentials for biological cells are usually treated using the *diffusion potential* approach [54] [55], where it is assumed that the observed transmembrane potential (often designated as "membrane potential") is equal to the thermodynamic diffusion potential. However, an undesirable outcome of this approach is the emergence of negative permeability coefficients, which are unrealistic [56]. Ohki [57] [58], and MacDonald and Bangham [59] were the first to include the contribution of surface potentials to the observed transmembrane potential of biomembranes. Ohki presented experimental observations, accompanied by theoretical calculations, in seeking to clarify the relation between surface potentials, diffusion potential and transmembrane potential [56]. Surface potentials arise from the presence of charged groups at the outer (extracellular medium) and inner (cytoplasmic) surfaces of the plasma membrane. As described above, the negative charge at the outer cell membrane surface is primarily due to membrane-bound, ionized carboxyl groups of sialic acid residues.

Consistent with the above discussions, we focus our attention on the outer cell surface charge and its resultant electric potential.

The characteristic Debye length of surface potentials for cells is of the order of 1 nm [60], so there is no possibility of resolving surface potentials from diffusion potentials. The surface potential at the inner (cytoplasmic) surface of a membrane is also primarily due to anionic groups [56] [61]. Additionally, polarization potentials V_p from polarized molecules at the inner and outer surfaces of the membrane arise from surface molecules possessing dipole moments. It will be assumed here that the polarization potentials at membrane surfaces effectively cancel each other [56]. Thus, for the measured transmembrane potential, ΔV_m, we have

$$\Delta V_m = \varphi_i + \varphi_o + V_d \tag{5}$$

where V_d is (if φ_i and φ_o are 0) the diffusion potential arising from unequal ionic concentrations between the inside and outside of a cell, and φ_i and φ_o are the surface potentials at the cytoplasmic (inner), and extracellular (outer) cell membrane surfaces, respectively. Because of the surface electric potentials, the actual potential associated with the passive diffusion of ions is ΔV_m, not V_d. To simplify, V_d will be designated as the intramembrane potential in the presence of surface potentials, and as the diffusion potential in the absence of surface potentials; both are intramembrane electric potentials. Due to the increased outer surface membrane-bound negative charge described above, a larger negative surface potential (**Figure 2**) will exist at the outer surface of cancer cells.

The Nernst potential V_N [62] of an ion in pure passive electrodiffusive equilibrium (no ion pumps) across a cell membrane is given by

$$V_N = -(kT/Ze)\ln(C_i/C_o) \tag{6}$$

where C_i/C_o is the ratio of the ion's concentration inside vs. outside the cell, Z is the valence of the ion, e is the magnitude of the charge on an electron, k is

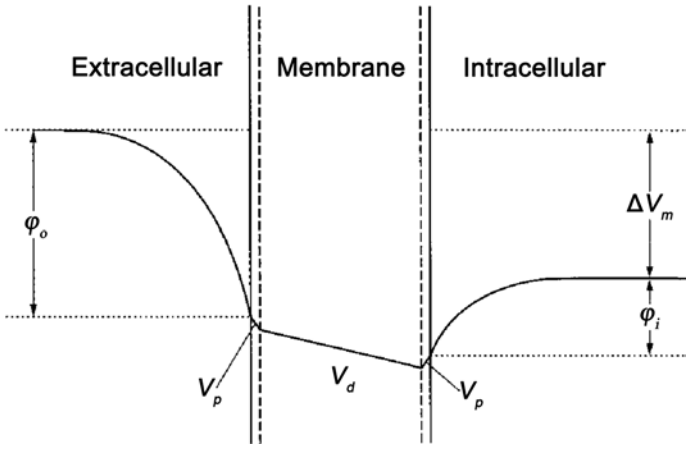

Figure 2. Schematic transmembrane electric potential profile. Surface potentials φ_i and φ_o are shown in relation to the intramembrane potential V_d. The polarization potentials V_p and the measured trans-membrane potential ΔV_m are also depicted as described in the text.

Boltzmann's constant, and T is absolute temperature. The Nernst potentials of each of the ions in passive electrodiffusive equilibrium must be equal.

For a given potential difference $(C_i/C_o)^{1/Z}$ is the same for all ions. Thus, for monovalent cations and anions ($Z = \pm 1$), we have

$$C_{i(+)}/C_{o(+)} = C_{o(-)}/C_{i(-)} \tag{7}$$

where $C_{i(-)}$ and $C_{i(+)}$ are the intracellular concentrations of negatively and positively charged permeant ions, respectively, with a similar notation for extracellular ions. Concentrations of ions in the extracellular medium and the total concentration of intracellular impermeant ions C_{np}, along with (7) and the bulk intracellular electroneutrality condition are sufficient to determine the concentrations of permeant ions in the cell in the absence of active transport.

A considerable body of research identifies a relationship among intracellular ionic concentrations, cell membrane electric potential and mitogenesis. Mitotically active cells are often found to have low (−10 to −20 mV) transmembrane potentials and altered concentrations of monovalent ions such as sodium, potassium and chloride [27] [63] [64]. For example, a significant rise in intracellular sodium in highly differentiated neurons has been associated with the initiation of DNA synthesis [63]. This is particularly significant since cell electric potential and sodium ion concentration have also been associated with contact inhibition in monolayer cell cultures [65].

Primitive cells had to divide with very few biological mechanisms in place. It is therefore doubtful that their membranes had the requisite carrier molecules needed for active transport. Thus, it will be assumed here that the earliest dividing cells did not possess ion pumps. It is further assumed that a reasonable approximation for the transmembrane potential may be obtained by considering the monovalent ions K^+, Na^+ and Cl^- along with experimental values for the intracellular concentrations of impermeant ions. This assumption is revisited below in light of experimental data on actual cell membrane potentials.

It is reasonable to assume that repeated cell division was not only a necessity but also natural for the first successful primitive cells, and it was only later that systems of cells, such as those found in multicellular organisms, evolved "social controls" over cell division. It has been suggested that a loss of such controls is at least partially responsible for the neoplastic transformation. The loss of social control has a simple interpretation in the context of the present work regarding electrostatic considerations.

Following Benedek and Villars [66], we calculate the intracellular concentrations of sodium, potassium and chloride ions in pure passive electrodiffusive equilibrium, as it is assumed here to have been the situation for individual, isolated primitive cells whose existence depended on continuing cell division with no social controls. Typical experimental values of extracellular concentrations of potassium, sodium and chloride ions are 10, 140 and 150 mM, respectively. These values, along with an intracellular nonpermeant ion concentration C_{np} of 125 mM [66] may be substituted into

$$C_{K(i)}/C_{K(o)} = C_{Na(i)}/C_{Na(o)} \quad \text{and} \quad C_{Na(i)}/C_{Na(o)} = C_{Cl(o)}/C_{Cl(i)} \tag{8}$$

satisfying the requirement of overall intracellular electrical neutrality

$$C_{K(i)} + C_{Na(i)} = C_{Cl(i)} + C_{np} \tag{9}$$

to obtain intracellular concentrations of potassium, sodium and chloride ions of 15, 210 and 100 mM, respectively. The transmembrane potential is then given from (6) as −11 mV at T = 310 K (body temperature). Such values for the cell potential and ionic concentrations are typical of present-day mitotically active cells.

The above calculation will be repeated with the inclusion of active pumping of sodium ions from the cell to the extracellular medium. Experimentally, the active transport of sodium ions results in an intracellular sodium concentration of 12 mM. Using this value for the intracellular sodium ion concentration, along with the same values for the extracellular concentrations of sodium, potassium and chloride ions from the previous calculation, and the same intracellular concentration C_{np} of impermeant ions, application of the equality of the Nernst potentials (6) for potassium and chloride ions, and electrical neutrality (9) to all three ions, yields 125 mM and 12 mM for the intracellular concentrations of potassium and chloride ions, respectively. These values satisfy the condition:

$$C_{K(i)}/C_{K(o)} = C_{Cl(o)}/C_{Cl(i)} = 12.5 \tag{10}$$

as well as intracellular electroneutrality. Since electrodiffusive equilibrium applies to potassium and chloride ions, the Nernst potentials of these ions are equal:

$$V_N\left(\mathrm{K}^+\right) = V_N\left(\mathrm{Cl}^-\right) \tag{11}$$

Thus we have:

$$\left(-kT/Ze\right)\ln\left(C_{K(i)}/C_{K(o)}\right) = \left(kT/Ze\right)\ln\left(C_{Cl(i)}/C_{Cl(o)}\right) \tag{12}$$

And from the equality of concentration ratios given in (10), we have $V_N(\mathrm{K}^+) = V_N(\mathrm{Cl}^-) = -67$ mV at T = 310 K. This transmembrane potential value compares favorably to experimental values for non-dividing cells [63].

The cytosolic and nucleoplasmic *ionic strength*

$$I = (1/2)\sum M_n Z_n^2 \tag{13}$$

where M_n is the *molal* concentration, and Z_n the ionic valence, will also be permanently different for cancer cells. This important difference will be considered below in the context of DNA replication.

4. Cell Membrane Charge, Intramembrane Potential, Ion Concentrations and Cancer

The calculation above reveals that a significantly smaller transmembrane potential (as observed in cancerous cells; [27] [28]) is consistent with an impaired, or absent, plasma membrane sodium pump in cycling cells. In accord with experiment [63], the calculation is in agreement with increased sodium ion

intracellular concentration for malignant cells. Note that the observed temporary drop in transmembrane potential during mitosis for many normal cell types is not being addressed here (but see below).

Primitive biological cells likely lacked the intramembrane carrier molecules needed for active sodium *export* from cells (e.g., Na^+/K^+-ATPase pumps), thus it is reasonable to assume that the natural and necessary tendency for the uncontrolled cell division of ancient, unicellular organisms occurred within conditions of passive electrodiffusive equilibrium without active pumping. With the arrival of photosynthesis, planetary oxygen and multicellular organisms, the need for social controls over cell division likely required the evolution of Na^+/K^+ plasma membrane pumps consistent with the large (negative) transmembrane electric potentials observed in non-cycling cells, along with the above calculated, and experimentally confirmed, ion concentrations characteristic of such cells. In multicellular organisms, these ionic concentrations are shared among large numbers of cells due to normally functioning gap junctions. A large volume of cells freely sharing non-mitogenic concentrations of ions is integral to an organism's social control over cell division, and thus increased cell surface negative charge likely compromises proper gap junction formation and the consequent maintenance of non-mitogenic ionic concentrations in multicellular organisms.

In modern cells, the carrier molecules necessary for the active transport of sodium reside within the cell membrane, and therefore sense only the intramembrane potential portion of the transmembrane electric potential [67]. From (5), the transmembrane potential ΔV_m is the sum of the surface potentials at the outer and inner surfaces and the intramembrane voltage V_d. This equation is key to understanding a possible role for increased negative charge at the cell surface in cancer cell mitogenesis.

Since an increased density of negatively charged sialic acid residues σ at the outer cell membrane of cancer cells will produce a greater negative surface electric potential φ_o, it follows from (5) that for a given measured ΔV_m there must be a corresponding decrease in the magnitude (smaller negative value) or a positive value for the intramembrane potential V_d, relative to normal values [67] [68]. Measurements of transmembrane potentials are unable to resolve the potentials φ_o and φ_i, and reflect only the total potential drop across the membrane, ΔV_m (**Figure 2**), which is due solely to the *bulk* concentrations of ions in the extracellular environment and in the cytosol. This is a consequence of the Boltzmann energy distribution function of classical statistical mechanics, which governs the dependence of the total potential change (the transmembrane potential) between bulk medium extracellular and intracellular ion concentrations under electrodiffusive equilibrium conditions. In addition, given that the transmembrane potential is permanently lower in magnitude (less negative) for cancerous cells, it follows that the intramembrane potential is likely positive, zero or slightly negative. This combination of conditions give sufficient basis to assume that the carrier molecules responsible for active transport of sodium ions out of a cell (*ex-*

port) will sense a significantly altered intramembrane potential—as well as increased membrane electrical stress—likely affecting active sodium ion export as well as the operation of ion channels [67]. This modification of the plasma cell membrane ion transport properties of cancer cells likely has important consequences for mitogenesis (see below).

An increasing number of studies suggest that ion channels and pumps are important players in cell proliferation [69]. As demonstrated in the above calculation, the reduced transmembrane potential characteristic of cancer cells is consistent with an increased intracellular sodium ion concentration resulting from impaired—or absent—plasma membrane sodium/potassium (Na^+/K^+-ATPase) active pumping. Note that several studies show that $[Na^+]$ is significantly elevated in cancer cells [27] [70].

Experiments have revealed that the transient movement of sodium ions into cells is associated with a rise of intracellular pH (pH_i) that occurs when many cell types leave division arrest [71], and that a large drop in transmembrane potential occurs as cells enter mitosis [27]. It is therefore reasonable to assume that a sustained, increased intracellular sodium ion concentration, as well as a sustained lower transmembrane potential (as observed in mitotically active and cancer cells) would cause a permanently elevated pH_i due to Na^+/H^+ exchange [71] [72] [73] and the electrostatic requirement of intracellular electrical neutrality. Significantly, observations have revealed that cytoplasmic and nuclear pH are equivalent in HeLa cells [74], a well-known line of cancer cells. Alkaline pH appears to be a necessary preparatory condition for DNA synthesis [75], and studies have shown that intracellular acidification can diminish tumor growth and provoke cytotoxic death [76].

The conditions described here—1) low transmembrane potential, 2) impaired or absent Na^+/K^+ plasma membrane pumps, 3) high intracellular sodium ion concentration, and 4) alkaline cellular pH_i—are consistent with the reversion of cells to a more primitive mitotically active, cancerous lifestyle. In accord with experiment, the calculations above directly support the first three of these conditions, and given a high intracellular sodium ion concentration, condition (4) follows due to H^+/Na^+ exchange [71] and overall electrical neutrality.

As alluded to above, the commonly observed transient influx of sodium ions and the temporary drop in transmembrane potential during normal cell division is not to be confused with the permanently lowered mitogenic intramembrane potential—with consequent failure of sodium ion active pumping—and permanently increased $[Na^+]$ discussed here. We propose that this observation is consistent with the present discussion as follows. During mitosis, the mitotic apparatus occupies most of the volume of the cell, and mitochondrial, as well as other inner membranes, disassemble into membrane fragments, likely due to increased electrostatic stress during mitosis. A full analysis of this process for the membranes of the nuclear envelope is given elsewhere [2]. Thus it seems reasonable that mitochondrial functioning to provide the ATP necessary for active pumping

is not operative during mitosis. Consequently, the absence of Na^+/K^+ pumping leads to electrodiffusive equilibrium conditions, including observations of low transmembrane potential and the movement of sodium ions into cells.

It is well-known that ionic strength is significant in the biochemical reactions within polyelectrolytes like the cytoplasm of biological cells. Ionic strength calculations, based on ion concentrations in cancer cells as compared to normal counterparts, reveal that the cytosolic and nucleoplasmic ionic strengths of cancerous cells are considerably higher. Data from Cameron *et al.* [70] reveals that the cytoplasmic ratio of ionic strength for cancer cells relative to their normal counterparts is 1.6. Ionic strength relates to the degree of shielding of electrostatic interactions in an ionic medium. Thus it seems that the greater cytoplasmic and nucleoplasmic ionic strengths of cancer cells are significant for the protein biochemistry of these cells.

Experiments reveal that the optimum pH for DNA synthesis is a strong function of ionic strength [77] [78], likely due to the dependence of hydrogen bond strength on the amount of electrostatic shielding. For a polycationic environment surrounding an enzyme, the pH optimum will be shifted toward more acidic values; a shift toward more basic values occurs in a polyanionic environment [78]. For example, experiments show that, in RNA systems (with similar results expected for DNA systems) a polycationic ionic strength ratio of 1.5 results in an optimum pH shift from 8.3 to 7.5 [78]. As noted, the cytosolic ratio of ionic strengths for cancer cells relative to non-cancer cells is 1.6, with an expectation that nucleoplasmic ratios should be commensurate with this ratio. Thus it is reasonable to expect significant alterations in the DNA biochemistry of cancer cells, causing DNA synthesis to occur when it should not.

It is generally thought that once DNA replication is initiated, a cell is committed to divide. However not much is offered in the biological literature to explain the link between replication and the events of mitosis (nuclear division). Here we propose that the sudden "explosion" in the demand for protons needed for DNA replication (*i.e.*, the rapid conversion of uracil to thymidine via the thymidylate synthase salvage pathway during S phase [79]) soon depletes nuclear proton stores, causing a "proton-poor" nucleoplasm. The subsequent increased *local* pH in the extranuclear environment, and consequent increase in nuclear membrane electrostatic stress (ES), leads to fragmentation of the nuclear envelope membranes [2]. The further spread [80] of the proton-poor condition leads to the cytosolic alkalinization observed during early prophase [81] [82]; subsequently, a steadily decreasing pH_i during mitosis acts as a master clock for the timing of chromosome motions during mitosis [83] [84].

5. Conclusions

Increased cell surface negative charge—membrane-bound, ionized carboxyl groups of sialic acid residues—is directly correlated with a number of characteristics of cancer cells. The present work relates to increased cell surface negative

charge to aspects of mitogenesis in cancer cells including increased membrane electrostatic stress (via sialic acid) and reduced intramembrane electric potential. Both are associated with altered cytoplasmic and nucleoplasmic ionic concentrations likely integral to mitogenesis. As supported by the experiment as well as calculation, the loss of active Na^+/K^+ plasma membrane pumping is consistent with increased concentrations of sodium and other ions, low trans- and intramembrane electric potential, and alkaline cytoplasmic pH, all related to mitogenesis. Increased ionic concentrations, with attendant increased ionic strength, may result in modifications in electrostatic interactions of proteins (e.g., cell cycle checkpoints) and nucleic acids through altered charge screening, leading to conditions favoring DNA synthesis and subsequent aberrant cell division.

Abnormal cells exhibit greatly increased intercellular electrical resistance, a condition that is consistent with increased surface charge and the consequent observed electrical isolation of malignant cells. This negates the power of large cell assemblies to equalize their ionic concentrations (social control) through normally functioning gap junctions, thus allowing ionic concentrations with mitogenic potential. A failure of ionic continuity at the peripheries of abnormal, electrically isolated cells with mitogenic intracellular ionic concentrations would allow cancerous cells to grow within normal surrounding tissue (a situation not unlike the conditions for isolated unicellular organisms), a common observation in the histology of tumors.

Ethics Approval and Consent to Participate

Not applicable.

Consent for Publication

Not applicable.

Availability of Data and Materials

Not applicable.

Funding

Busch Biomedical grant to DHS.

Authors' Contributions

LJG conceptualized the theoretical aspects of this article and DHS provided intellectual contributions. Both authors read and approved the final manuscript.

Acknowledgments

Not applicable.

Conflicts of Interest

The authors declare no conflicts of interest regarding the publication of this paper.

References

[1] Gagliardi, L.J. (2005) Electrostatic Force Generation in Chromosome Motions during Mitosis. *Journal of Electrostatics*, **63**, 309-327. https://doi.org/10.1016/j.elstat.2004.09.007

[2] Gagliardi, L.J. (2006) Electrostatic Considerations in Nuclear Envelope Breakdown and Reassembly. *Journal of Electrostatics*, **64**, 843-849. https://doi.org/10.1016/j.elstat.2006.02.005

[3] Gagliardi, L.J. and Shain, D.H. (2014) Polar Electrostatic Forces Drive Poleward Chromosome Motions. *Cell Division*, **9**, 5. https://doi.org/10.1186/s13008-014-0005-3

[4] Gagliardi, L.J. and Shain, D.H. (2014) Chromosome Congression Explained by Nanoscale Electrostatics. *Theoretical Biology and Medical Modelling*, **11**, Article No. 12. https://doi.org/10.1186/1742-4682-11-12

[5] Gagliardi, L.J. and Shain, D.H. (2016) Electrostatic Forces Drive Poleward Chromosome Motions at Kinetochores. *Cell Division*, **11**, 14. https://doi.org/10.1186/s13008-016-0026-1

[6] van Beek, W.P., Smets, L.A. and Emmelot, P. (1973) Increased Sialic Acid Density in Surface Glycoprotein of Transformed and Malignant Cells—A General Phenomenon? *Cancer Research*, **33**, 2913-2922.

[7] Seaman, G.V.F. and Cook, G.M.W. (1965) Modification of the Electrophoretic Behaviour of the Erythrocyte by Chemical and Enzymatic Methods. In: Ambrose, E.J., Ed., *Cell Electrophoresis*, J & A Churchill Ltd., London, 48-65.

[8] Sand, S.L., Nissen-Meyer, J., Sand, O. and Haug, T.M. (2013) Plantaricin A, a Cationic Peptide Produced by *Lactobacillus plantarum*, Permeabilizes Eukaryotic Cell Membranes by a Mechanism Dependent on Negative Surface Charge Linked to Glycosylated Membrane Proteins. *Biochimica et Biophysica Acta Biomembranes*, **1828**, 249-259. https://doi.org/10.1016/j.bbamem.2012.11.001

[9] Du, J., Meledeo, M.A., Wang, Z., Kanna, H.S., Paruchuri, V.D.P. and Yarema, K.J. (2009) Metabolic Glycoengineering: Sialic Acid and Beyond. *Glycobiology*, **19**, 1382-1401. https://doi.org/10.1093/glycob/cwp115

[10] Tamura, A., Morita, K., Fujii, T. and Kojima, K. (1982) Detection of the Electrical Surface Charge Induced by Treatment of the Membrane Lipid Bilayer of Human Erythrocytes. *Cell Structure and Function*, **7**, 21-27. https://doi.org/10.1247/csf.7.21

[11] Corfield, A. (2017) Eukaryotic Protein Glycosylation: A Primer for Histochemists and Cell Biologists. *Histochemistry and Cell Biology*, **147**, 119-147. https://doi.org/10.1007/s00418-016-1526-4

[12] Weiss, L. and Mayhew, E. (1969) Ribonuclease-susceptible Charged Groups at the Surface of Ehrlich Ascites Tumour Cells. *International Journal of Cancer*, **4**, 626-635. https://doi.org/10.1002/ijc.2910040507

[13] Wolstenholme, G.E.W. and Knight, J. (1971) Growth Control in Cell Cultures. Churchill Livingstone, Edinburgh.

[14] Buck, C.A., Glick, M.C. and Warren, L. (1971) Glycopeptides from the Surface of Control and Virus-Transformed Cells. *Science*, **172**, 169-171. https://doi.org/10.1126/science.172.3979.169

[15] Warren, L., Fuhrer, J.P. and Buck, C.A. (1972) Surface Glycoproteins of Normal and Transformed Cells: A Difference Determined by Sialic Acid and a Growth-Dependent Sialyl Transferase. *Proceedings of the National Academy of Sciences*, **69**, 1838-1842.

https://doi.org/10.1073/pnas.69.7.1838

[16] Loewenstein, W.R. and Kanno, Y. (1966) Intercellular Communication and the Control of Tissue Growth: Lack of Communication between Cancer Cells. *Nature*, **209**, 1248-1249. https://doi.org/10.1038/2091248a0

[17] Fedarko, N.S., Ishihara, M. and Conrad, H.E. (1989) Control of Cell Division in Hepatoma Cells by Exogenous Heparan Sulfate Proteoglycan. *Journal of Cellular Physiology*, **139**, 287-294. https://doi.org/10.1002/jcp.1041390210

[18] Baserga, R. (1965) The Relationship of the Cell Cycle to Tumor Growth and Control of Cell Division: A Review. *Cancer Research*, **25**, 581-595.

[19] Cormack, D. (1970) Effect of Enzymatic Removal of Cell Surface Sialic Acid on the Adherence of Walker 256 Tumor Cells to Mesothelial Membrane. *Cancer Research*, **30**, 1459-1466.

[20] Bassaganas, M., Perez-Garay, M. and Peracaula, R. (2012) Adhesive and Migratory Behaviour of Pancreatic Adenocarcinoma Capan-1 Cells Is Regulated by Changes in Sialic Acid of Alpha2beta1 Integrin. *European Journal of Cancer*, **48**, S57. https://doi.org/10.1016/S0959-8049(12)70927-9

[21] Bassaganas, S., Perez-Garay, M. and Peracaula, R. (2014) Cell Surface Sialic Acid Modulates Extracellular Matrix Adhesion and Migration in Pancreatic Adenocarcinoma Cells. *Pancreas*, **43**, 109-117. https://doi.org/10.1097/MPA.0b013e31829d9090

[22] Shanmugam, V., Chackalaparampil, I., Kundu, G.C., Mukherjee, A. and Mukherjee, B.B. (1997) Altered Sialylation of Osteopontin Prevents Its Receptor-Mediated Binding on the Surface of Oncogenically Transformed tsB77 Cells. *Biochemistry*, **36**, 5729-5738. https://doi.org/10.1021/bi961687w

[23] Gasic, G. and Gasic, T. (1962) Removal of Sialic Acid from the Cell Coat in Tumor Cells and Vascular Endothelium, and Its Effects on Metastasis. *Proceedings of the National Academy of Sciences of the United States of America*, **48**, 1172-1177. https://doi.org/10.1073/pnas.48.7.1172

[24] Kemp, R.B. (1968) Effect of the Removal of Cell Surface Sialic Acids on Cell Aggregation *in Vitro*. *Nature*, **218**, 1255-1256. https://doi.org/10.1038/2181255a0

[25] Benedetti, E.L. and Emmelot, P. (1976) Studies on Plasma Membranes. *Journal of Cell Science*, **2**, 499-512.

[26] Roth, S. and White, D. (1972) Intercellular Contact and Cell-Surface Galactosyl Transferase Activity. *Proceedings of the National Academy of Sciences of the United States*, **69**, 485-489. https://doi.org/10.1073/pnas.69.2.485

[27] Cone, C.D. (1971) Unified Theory on the Basic Mechanism of Normal Mitotic Control and Oncogenesis. *Journal of Theoretical Biology*, **30**, 151-181. https://doi.org/10.1016/0022-5193(71)90042-7

[28] Cone, C.D. (1971) Maintenance of Mitotic Homeostasis in Somatic Cell Populations. *Journal of Theoretical Biology*, **30**, 183-194. https://doi.org/10.1016/0022-5193(71)90043-9

[29] Levin, M. (2012) Molecular Bioelectricity in Developmental Biology: New Tools and Recent Discoveries. *Bioessays*, **34**, 205-217. https://doi.org/10.1002/bies.201100136

[30] Gurtovenko, A.A. and Vattulainen, I. (2009) Intrinsic Potential of Cell Membranes: Opposite Effects of Lipid Transmembrane Asymmetry and Asymmetric Salt Ion Distribution. *Journal of Physical Chemistry B*, **113**, 7194-7198. https://doi.org/10.1021/jp902794q

[31] Shaefer, H. and Schanne, O. (1956) Membranpotentiale von Einzelzellen in Gewe-

bekulturen. *Naturwissenschafften*, **43**, 445. https://doi.org/10.1007/BF00629508

[32] Tokuoka, S. and Morioka, H. (1957) The Membrane Potential of the Human Cancer and Related Cells. *Gann*, **48**, 353-354.

[33] Johnstone, B.M. (1959) Micro-Electrode Penetration of Ascites Tumour Cells. *Nature*, **183**, 411. https://doi.org/10.1038/183411a0

[34] Griffiths, D.J. (1999) Introduction to Electrodynamics. Prentice-Hall, Upper Saddle River, 103.

[35] Weiss, L. (1968) Studies on Cell Deformability: V. Some Effects of Ribonuclease. *Journal of Theoretical Biology*, **18**, 9-18. https://doi.org/10.1016/0022-5193(68)90167-7

[36] Bockris, J.O. and Reddy, A.K.N. (1977) Modern Electrochemistry. Plenum Press, New York.

[37] Teschke, O., Ceotto, G. and de Souza, E.F. (2001) Interfacial Water Dielectric-Permittivity Profile Measurements Using Atomic Force Microscopy. *Physical Review E*, **64**, Article ID: 011605. https://doi.org/10.1103/PhysRevE.64.011605

[38] Pashley, R.M. (1981) DLVO and Hydration Forces between Mica Surfaces in Li^+, Na^+, K^+ and Cs^+ Electrolyte Solutions: A Correlation of Double-Layer and Hydration Forces with Surface Cation Exchange Properties. *Journal of Colloid and Interface Science*, **83**, 531-546. https://doi.org/10.1016/0021-9797(81)90348-9

[39] Heinz, W.F. and Hoh, J.H. (1999) Relative Surface Charge Density Mapping with the Atomic Force Microscope. *Biophysical Journal*, **76**, 528-538. https://doi.org/10.1016/S0006-3495(99)77221-8

[40] Giese, A.C. (1968) Cell Physiology. W.B. Saunders, Philadelphia, 104.

[41] Segal, J.R. (1968) Surface Charge of Giant Axons of Squid and Lobster. *Biophysical Journal*, **8**, 470-489. https://doi.org/10.1016/S0006-3495(68)86501-4

[42] Fettiplace, R., Andrews, D.M. and Haydon, D.A. (1971) The Thickness, Composition and Structure of Some Lipid Bilayers and Natural Membranes. *Journal of Membrane Biology*, **5**, 277-296. https://doi.org/10.1007/BF01870555

[43] Mayhew, E. (1966) Cellular Electrophoretic Mobility and the Mitotic Cycle. *The Journal of General Physiology*, **49**, 717-725. https://doi.org/10.1085/jgp.49.4.717

[44] Mayhew, E. and O'Grady, E.A. (1965) Electrophoretic Mobilities of Tissue Culture Cells in Exponential and Parasynchronous Growth. *Nature*, **207**, 86-87. https://doi.org/10.1038/207086a0

[45] Glick, M.C., Gerner, E.W. and Warren, L. (1971) Changes in the Carbohydrate Content of the KB Cell during the Growth Cycle. *Journal of Cellular Physiology*, **77**, 1-5. https://doi.org/10.1002/jcp.1040770102

[46] Anderson, A.P., Moreira, J.M.A. and Pedersen, S.F. (2014) Interactions of Ion Transporters and Channels with Cancer Cell Metabolism and the Tumour Environment. *Philosophical Transactions of the Royal Society B*, **369**, Article ID: 20130098. https://doi.org/10.1098/rstb.2013.0098

[47] Alberts, B., Bray, D., Lewis, J., Raff, M., Roberts, K. and Watson, J.D. (1994) Molecular Biology of the Cell. 3rd Edition, Garland Publishing, New York, 1077.

[48] Kemp, R.B. (1970) The Effect of Neuraminidase (3:2:1:18) on the Aggregation of Cells Dissociated from Embryonic Chick Muscle Tissue. *Journal of Cell Science*, **6**, 751-766.

[49] Morell, A.G., Gregoriades, G., Scheinberg, I.H., Hickman, J. and Ashwell, G. (1971) The Role of Sialic Acid in Determining the Survival of Glycoproteins in the Circula-

tion. *Journal of Biological Chemistry*, **246**, 1461-1467.

[50] Woodruff, J.J. and Gesner, B.B. (1969) The Effect of Neuraminidase on the Fate of Transfused Lymphocytes. *Journal of Experimental Medicine*, **129**, 551-567. https://doi.org/10.1084/jem.129.3.551

[51] Culp, L.A., Grimes, W.J. and Black, P.H. (1971) Contact Inhibited Revertant Cell Lines Isolated from SV40-Transformed Cells. *Journal of Cell Biology*, **50**, 682-690. https://doi.org/10.1083/jcb.50.3.682

[52] Perdue, J.F., Kletzien, R. and Wray, V.L. (1972) The Isolation and Characterization of Plasma Membrane from Cultured Cells: IV. The Carbohydrate Composition of Membranes Isolated from Oncogenic RNA Virus-Converted Chick Embryo Fibroblasts. *Biochimica et Biophysica Acta Biomembranes*, **266**, 505-510. https://doi.org/10.1016/0005-2736(72)90106-X

[53] Vaheri, A., Ruoslahti, E. and Nordling, S. (1972) Neuraminidase Stimulates Division and Sugar Uptake in Density-Inhibited Cell Cultures. *Nature New Biology*, **238**, 211-212. https://doi.org/10.1038/newbio238211a0

[54] Goldman, D.E. (1943) Potential, Impedance, and Rectification in Membranes. *Journal of General Physiology*, **27**, 37-60. https://doi.org/10.1085/jgp.27.1.37

[55] Hodgkin, A.L. and Katz, B. (1949) The Effect of Sodium Ions on the Electrical Activity of the Giant Axon of the Squid. *Journal of Physiology*, **108**, 37-77. https://doi.org/10.1113/jphysiol.1949.sp004310

[56] Ohki, S. (1981) Membrane Potential, Surface Potential, and Ionic Permeabilities. *Physiological Chemistry and Physics*, **13**, 195-210.

[57] Ohki, S. (1971) Electrical Potential of an Asymmetric Membrane. *Journal of Colloid and Interface Science*, **37**, 318-324. https://doi.org/10.1016/0021-9797(71)90299-2

[58] Ohki, S. (1972) Membrane Potential of Phospholipid Bilayers: Ion Concentration and pH Difference. *Biomembranes*, **282**, 55-71. https://doi.org/10.1016/0005-2736(72)90310-0

[59] MacDonald, R.C. and Bangham, A.D. (1972) Comparison of Double Layer Potentials in Lipid Monolayers and Lipid Bilayer Membranes. *Journal of Membrane Biology*, **7**, 29-53. https://doi.org/10.1007/BF01867908

[60] Hille, B., Woodhull, A.M. and Shapiro, B.I. (1975) Negative Surface Charge near Sodium Channels of Nerve: Divalent Ions, Monovalent Ions, and pH. *Philosophical Transactions of the Royal Society of London. Series B, Biological Sciences*, **270**, 301-318. https://doi.org/10.1098/rstb.1975.0011

[61] Hille, B. (2001) Ion Channels of Excitable Membranes. Sinauer, Sunderland, 656.

[62] Hille, B. (2001) Ion Channels of Excitable Membranes. Sinauer, Sunderland, 15.

[63] Stillwell, E.F., Cone, C.M. and Cone, C.D. (1973) Stimulation of DNA Synthesis in CNS Neurones by Sustained Depolarisation. *Nature New Biology*, **246**, 110-111. https://doi.org/10.1038/newbio246110a0

[64] McDonald, T.F., Sachs, H.G., Orr, C.W. and Ebert, J.D. (1972) External Potassium and Baby Hamster Kidney Cells: Intracellular Ions, ATP, Growth, DNA Synthesis and Membrane Potential. *Developmental Biology*, **28**, 290-303. https://doi.org/10.1016/0012-1606(72)90145-5

[65] Cone, C.D. and Tongier, M. (1973) Contact Inhibition of Division: Involvement of the Electrical Transmembrane Potential. *Journal of Cellular Physiology*, **82**, 373-386. https://doi.org/10.1002/jcp.1040820307

[66] Benedek, G.B. and Villars, F.M.H. (2000) Physics: With Illustrative Examples from Medicine and Biology: Electricity and Magnetism. Springer Verlag, New York, 478.

https://doi.org/10.1007/978-1-4612-1228-7

[67] Hille, B. (2001) Ion Channels of Excitable Membranes. Sinauer, Sunderland, 646-657.

[68] Van der Kloot, W.G. and Cohen, I. (1979) Membrane Surface Potential Changes May Alter Drug Interactions: An Example, Acetylcholine and Curare. *Science*, **203**, 1351-1352. https://doi.org/10.1126/science.424757

[69] Litan, A. and Langhans, S. (2015) Cancer as a Channelopathy: Ion Channels and Pumps in Tumor Development and Progression. *Frontiers in Cellular Neuroscience*, **9**, 86. https://doi.org/10.3389/fncel.2015.00086

[70] Cameron, I.L., Smith, K.R. and Skehan, P. (1982) Energy Dispersive Spectroscopy in the Study of the Ionic Regulation of Growth in Normal and Tumor Cells. *Proceedings of the Symposium on Ions, Cell Proliferation, and Cancer*, Essex, 13-40. https://doi.org/10.1016/B978-0-12-123050-0.50007-2

[71] Wolfe, S.L. (1993) Molecular and Cellular Biology. 2nd Edition, Wadsworth, Belmont, 920.

[72] Alberts, B., Bray, D., Hopkin, K., Johnson, A., Lewis, J., Raff, M., Roberts, K. and Walter, P. (2010) Essential Cell Biology. Third Edition, Garland Science, New York, 401.

[73] Moolenaar, W.H., de Laat, S.W., Mummery, C. and van der Saag, P.T. (1982) Na^+/H^+ Exchange in the Action of Growth Factors. *Proceedings of the Symposium on Ions, Cell Proliferation, and Cancer*, Essex, 151-162. https://doi.org/10.1016/B978-0-12-123050-0.50015-1

[74] Selsek, O. and Bolard, J. (1996) Nuclear pH Gradient in Mammalian Cells Revealed by Microspectrofluorimetry. *Journal of Cell Science*, **109**, 257-262.

[75] McBrian, M.A., Behbahan, I.S., Ferrari, R., Su, T., Huang, T., Li, K., Hong, C.S., Christofk, H.R., Vogelauer, M., Seligson, D.B. and Kurdistani, S.K. (2013) Histone Acetylation Regulates Intracellular pH. *Molecular Cell*, **49**, 310-321. https://doi.org/10.1016/j.molcel.2012.10.025

[76] Garcia-Canero, R., Trilla, C., Perez de Diego, Dıaz-Fil, J.J. and Cobo, J.M. (1999) Na^+:H^+ Exchange Inhibition Induces Intracellular Acidosis and Differentially Impairs Cell Growth and Viability of Human and Rat Hepatocarcinoma Cells. *Toxicology Letters*, **106**, 215-228. https://doi.org/10.1016/S0378-4274(99)00072-7

[77] Byrnes, J.J., Downey, K.M. and So, A.G. (1973) Bone Marrow Cytoplasmic Deoxyribonucleic Acid Polymerase. Variation of pH and Ionic Environment as a Possible Control Mechanism. *Biochemistry*, **12**, 4378-4384. https://doi.org/10.1021/bi00746a013

[78] Maurel, P. and Douzou, P. (1978) Cation-Induced Regulatory Mechanism of Enzyme Reactions. In: *Frontiers in Physicochemical Biology*, Academic Press, New York, 421-457. https://doi.org/10.1016/B978-0-12-566960-3.50024-5

[79] Berg, J.M., Tymoczko, J.L. and Stryer, L. (2011) Biochemistry. 7th Edition, Palgrave Macmillan, London, 1026.

[80] Gagliardi, L.J. (1973) A Possible Mechanism for Protonic Transfer in Aqueous Solutions. *Journal of Physical Chemistry*, **77**, 2098-2100. https://doi.org/10.1021/j100636a014

[81] Amirand, C., *et al.* (2000) Intracellular pH in One Cell Mouse Embryo Differs between Subcellular Compartments and between Interphase and Mitosis. *Biology of the Cell*, **92**, 409-419. https://doi.org/10.1016/S0248-4900(00)01080-7

[82] Steinhardt, R.A. and Morisawa, M. (1982) Changes in Intracellular pH of *Physarum*

plasmodium during the Cell Cycle and in Response to Starvation. In: Nuccitelli, R. and Deamer, D.W., Eds., *Intracellular pH*: *Its Measurement*, *Regulation*, *and Utilization in Cellular Functions*, Alan R. Liss, New York, 361-374.

[83] Gagliardi, L.J. and Shain, D.H. (2013) Is Intracellular pH a Clock for Mitosis? *Theoretical Biology and Medical Modelling*, **10**, 8. https://doi.org/10.1186/1742-4682-10-8

[84] Gagliardi, L.J. and Shain, D.H. (2018) Emergent Mitotic Chromosome Motions from a Changing Intracellular pH. *Open Journal of Biophysics*, **8**, 9-21. https://doi.org/10.4236/ojbiphy.2018.81002

Call for Papers

Open Journal of Biophysics

ISSN Print: 2164-5388 ISSN Online: 2164-5396
https://www.scirp.org/journal/ojbiphy

Open Journal of Biophysics (OJBIPHY) is an international journal dedicated to the latest advancement of biophysics. The goal of this journal is to provide a platform for scientists and academicians all over the world to promote, share, and discuss various new issues and developments in different areas of biophysics.

Subject Coverage

All manuscripts must be prepared in English, and are subject to a rigorous and fair peer-review process. Accepted papers will immediately appear online followed by printed hard copy. The journal publishes original papers including but not limited to the following fields:

- Bioelectromagnetics
- Bioenergetics
- Bioinformatics and Computational Biophysics
- Biological Imaging
- Biomedical Imaging and Bioengineering
- Biophysics of Disease
- Biophysics of Photosynthesis
- Cardiovascular Biophysics
- Cell Biophysics
- Medical Biophysics
- Membrane Biophysics
- Molecular Biophysics and Structural Biology
- Physical Methods
- Physiology and Biophysics of the Inner Ear
- Proteins and Nucleic Acids Biophysics
- Radiobiology
- Receptors and Ionic Channels Biophysics
- Sensory Biophysics and Neurophysiology
- Systems Biophysics
- Theoretical and Mathematical Biophysics

We are also interested in: 1) Short Reports—2-5 page papers where an author can either present an idea with theoretical background but has not yet completed the research needed for a complete paper or preliminary data; 2) Book Reviews—Comments and critiques.

Notes for Intending Authors

Submitted papers should not have been previously published nor be currently under consideration for publication elsewhere. Paper submission will be handled electronically through the website. All papers are refereed through a peer review process. For more details about the submissions, please access the website.

Website and E-Mail

https://www.scirp.org/journal/ojbiphy **E-mail: ojbiphy@scirp.org**

What is SCIRP?

Scientific Research Publishing (SCIRP) is one of the largest Open Access journal publishers. It is currently publishing more than 200 open access, online, peer-reviewed journals covering a wide range of academic disciplines. SCIRP serves the worldwide academic communities and contributes to the progress and application of science with its publication.

What is Open Access?

All original research papers published by SCIRP are made freely and permanently accessible online immediately upon publication. To be able to provide open access journals, SCIRP defrays operation costs from authors and subscription charges only for its printed version. Open access publishing allows an immediate, worldwide, barrier-free, open access to the full text of research papers, which is in the best interests of the scientific community.

- High visibility for maximum global exposure with open access publishing model
- Rigorous peer review of research papers
- Prompt faster publication with less cost
- Guaranteed targeted, multidisciplinary audience

Scientific Research Publishing

Website: https://www.scirp.org

Subscription: sub@scirp.org

Advertisement: service@scirp.org